THE EFFECTS OF SOLVENT DRAG AND SOLUTE DRAG ON DIFFUSION

by

Brent Chalmers

A THESIS

Presented to the Department of Biochemistry
and the Graduate Division of the School of Medicine,
University of Oregon Health Sciences Center,
in partial fulfillment of
the requirements for the degree of

Master of Science
June 1978

APPROVED: [redacted]

[redacted]

(Chairman, Graduate Council)

ACKNOWLEDGEMENTS

I wish to thank my advisor, Dr. J. T. Van Bruggen for his guidance and encouragement during my tenure as a graduate student. I also wish to thank Dr. Terry Mullen and Mrs. Mertie Muller for many hours of stimulating discussion and for making my experience in the laboratory an enjoyable one. Special thanks are extended to my wife, Barbara, for her invaluable assistance in the preparation of this manuscript and more importantly, for her unerring confidence in my intellectual abilities.

TABLE OF CONTENTS

LIST OF TABLES

LIST OF FIGURES

GLOSSARY OF SYMBOLS

J_v	Transmembrane volume flow.
J_s	Transmembrane solute flow.
ΔC	The difference in concentration of the two membrane bathing solutions.
$\overline{C}_s$	The mean concentration of the two membrane bathing solutions.
ΔP	The hydrostatic pressure difference of the two membrane bathing chambers.
P_s	The transmembrane flux of a solute at unit concentration difference and at zero net volume flow.
ω	The transmembrane flux of a solute at unit osmotic pressure difference and at zero net volume flow.
P	The transmembrane flux of a solute at unit concentration difference.
π	Osmotic pressure
σ	The Staverman reflection coefficient.
λ	Solute-solute flow interaction coefficient.
L_p	Hydraulic conductivity coefficient.
R	Ideal gas constant.
T	Temperature in degrees Kelvin.

How blind is he who cannot see

through a sieve.

--Cervantes (Don Quixote, Part II)

INTRODUCTION

In 1966 Ussing (1) reported some curious results of experiments on isolated frog skin. When the outside bathing solution was made hyperosmotic with respect to the inside bathing solution, a net flow of tracer sucrose from outside to inside occured. There was no concentration gradient for sucrose, and in the case where the skin was bathed in plain Ringer's solution, no net flow of sucrose occurred The effect was also demonstrated for sulfate ions, indicating that this "apparent active transport" was not specific for sucrose. Although Ussing postulated a role for active Na^+ transport, later experiments by himself (2) with ouabain and cyanide, and DNP in our laboratory (3) provided conclusive evidence that active transport of Na^+ was not involved in this new phenomena.

Almost simultaneously, Franz and Van Bruggen (4), while studying possible mechanisms of action of DMSO, observed similarly unusual asymmetric effects on movement of certain solutes across frog skin. Net influxes of several nonelectrolytes were demonstrated when the outside bathing solution contained 2.5% DMSO, this solution being hyperosmotic to normal bathing fluids. This effect was not specific for DMSO, but was found to be related to hypertonicity in general. Erythritol and thiourea hyperosmotic solutions in the outside bath caused net influxes of urea, mannitol and sucrose. Interestingly, hyperosmotic solutions of the nonpermeable sugar raffinose did not produce this net flux.

At the time, hyperosmotic solutions were known to have several effects on isolated frog skin (5,6). Lindley, Hoshiko and Leb (9) had

shown that if the outer bathing solution is made hyperosmotic with respect to the inside, skin potential and resistance invariably fall, these changes being dependent upon the nature and concentration of the solute. Ussing and Windhager (6) found a large decrease in skin resistance when the osmolarity of the outer bathing solution was doubled by the addition of urea to Na_2SO_4 Ringer's solution. These authors demonstrated this decrease in resistance to be due to an increase in the passive flux of sodium and sulfate ions through the skin via a "shunt pathway."

Franz and Van Bruggen (8) concluded that the hyperosmotic solutions have effects on solute movement that can be separated into two components. The first effect is related to the observation discussed in the preceeding paragraph. That is, hyperosmotic solutions change frog skin structure in such a way as to make the membrane more permeable to a variety of solutes. Since this increase in permeability affected solute movement in both directions, however, a second effect of hyperosmolarity must be postulated in order to explain a net movement of the solutes.

One theory as to how hypertonicity in the ouside bathing solution of frog skin could cause apparent active transfer of solutes has been presented by Ussing (10, 11). Ussing speculates that even though hypertonic solutions create a flow of water against the net movement of the transported solute, it may be that a sort of "backwater" of solvent is responsible for the actual carrying of solute in the inward direction. Called anomalous solvent drag, his model is dependent on certain ultrastructural characteristics of the frog skin epithelial cell that make the formation of this "backwater" possible. Specifically,

Ussing's "backwater" is located in the intercellular spaces, that is, between epithelial cells. The placement of the junctional complex at the apical region of the interspace is the crux of the model, for it is this structure that prevents a bulk flow of water in the outward direction, forcing water in the inward direction. Should solutes diffuse into this space, they would be carried by this inward flow. Ussing speculates this backwater is of sufficient magnitude to account for the apparent active transport he and others observed.

The special ultrastructural requirements of the anomalous solvent drag model immediately suggest experiments to test its validity. This model predicts that asymmetrical flows of solute could not be demonstrated in the reverse situation. That is, if the inner bathing solution of isolated frog skin were made hyperosmotic, a net flow of a tracer molecule, such as sucrose, from inside to outside should not occur. This experiment has been done by Biber and Curran (12), and a net flux in the inside to outside direction is detected under these conditions. These workers' data show that flux ratios[1] are comparable whether the hyperosmotic agent is in the inside or outside bathing solutions. On this basis, the contribution to flux asymmetries of "anomalous solvent drag" is probably not significant.

Franz and Van Bruggen (8) have presented a more straight forward interpretation of the phenomenon. These workers hypothesised that the hyperosmotic solute, as it diffuses across the membrane down its'

---

[1] flux ratio = $\frac{\text{flux of solute out of hyperosmotic solution}}{\text{flux of solute into hyperosmotic solution}}$

concentration gradient, transfers momentum to the tracer solute, for which there is no concentration gradient. The simplest explanation for this transfer of momentum is through direct frictional interaction between the two solutes when they are actually within the membrane. This model could explain the observation that hyperosmotic raffinose solutions fail to produce a net flux of tracer solute. Raffinose is too large a molecule to penetrate frog skin in appreciable amounts and thus would not be expected to participate in a momentum transfer. Apparently, actual movement of the hyperosmotic agent through the skin is a necessary part of the phenomena.

Franz and Van Bruggen were not the first to observe solute interaction. Work in free solution (13, 14, 15, 16) had shown that in a solution with two solutes, a concentration gradient for one of the solutes could cause movement of a second solute (one initially lacking a concentration gradient). The frog skin system differed only in that a membrane structure was interposed between solutions of unequal concentration and interaction was expressed in terms of transmembrane fluxes.

To further define the coupling of solute fluxes in membranes, Galey and Van Bruggen (17) studied interaction between a variety of solutes in artificial membranes. These systems had several advantages over live frog skin : 1) More precise experimentation was possible because one membrane could be used in many experiments. 2) Hydrostatic pressure could be applied to eliminate the effects of bulk water movement. 3) Interpretation of data is considerably simplified since more is known about the structure of the synthetic membranes than about the

structure of frog skin.

The results of Galey and Van Bruggen's work can be summarized as follows: 1) Interaction could be detected between a number of the solute pairs tested. 2) The larger the tracer solute for a given hyperosmotic agent the larger the flux asymmetrics seen. 3) For a given tracer, the observed flux asymmetrics generally did not increase with larger hyperosmotic agents. 4) The effectiveness of a hyperosmotic agent, as determined by an interaction coefficient, in creating asymmetric solute flow increased with smaller membrane pore radii.

These data can be readily explained by the notion that vectorial movement of hyperosmotic agent through a pore will create, through collision, the vectorial movement of a tracer solute also occupying the pore. If the solutes are larger, the cross sectional area available for interaction will be greater, so momentum transfer will be greater. The flow of larger hyperosmotic agents, however, will be restricted by the size of the pore, leading to less hyperosmotic agent actually diffusing through the membrane. This may explain why larger "driver" species do not necessarily cause larger flux ratios. Also, it is clear that a reduction in the pore size would restrict the randomness of solute interaction and thus increase the vectorial effect of the solute gradient, producing a more effective solute interaction per flux of hyperosmotic agent across the membrane.

As this point, another interpretation of Galey and Van Bruggan's results on artifical membranes described by Patlak and Rapoport (18) should be mentioned. These workers postulated that volume circulation, caused by the heteroporousity of the artifical membrane, could account for a net

movement of the tracer species under certain conditions.

To understand their theory, consider the system described below. A membrane separates two well stirred solutions. The tracer is on both sides and the hyperosmotic agent is on the right, to which a pressure is applied so that net volume flow due to osmotic pressure is eliminated. The membrane contains pores of different sizes, as do the artificial membranes used by previous workers. (3, 17). In this system, the reflection coefficient of the hyperosmotic solute will be smaller for the larger-than-average pores than it will for the smaller-than-average pores. This would suggest that there will be a net volume flow from left to right through the smaller-than-average pores and an equal volume flow in the opposite direction through the larger-than-average pores. This is the basis of the postulated "volume circulation" in heteroporous membranes (19, 20). To understand how this volume circulation could cause a net movement of tracer solute, consider that the amount of material a given volume flow will carry through a pore is related to the size of the pore. Thus, the larger pores (net flow in the right to left direction) will carry more tracer solute than the smaller pores (which have a net flow in the left to right direction). Overall, it can be seen that a net flow of tracer solute in the right to left direction will occur. This is the same direction that solute-solute interaction would cause tracer solute flux to occur.

In reality, little is known about pores and their size in heteroporous membranes. One can calculate approximations by the methods of Goldstein and Solomon (21) or Paganelli and Solomon (22), but these methods provide no information on true pore size distribution, area

available for solute flow, length of pore or the degree of tortuosity of the pore system. With the compressed "brush pile" configuration of cellulose acetate membranes, it may in fact be ambiguous to talk of pores at all. For these reasons, and to settle the question of what significance volume circulation might have on solute transfer on synthetic membranes, Van Bruggen et al (23) studied a newly developed homopore membrane. (For a description of this membrane see "Methods and Materials")

This work on the homopore membrane confirmed earlier observations on the heteropore membranes, and also permitted quantitative evaluation not possible on the older membrane. Interaction coefficients were calculated, and these values compared for the different solute pairs. As before, the largest interaction was noted to occur between solutes of the largest molecular size. Since volume circulation could not occur on a homopore membrane, these results seem to indicate that the solute-solute interaction model alone could adequately explain the net solute flow phenomena seen on heteroporous synthetic membranes. It was further determined that this interaction, termed "solute drag" by Van Bruggen et al could account for the in vitro observations by Ussing (1), Van Bruggen (4) and others (12,24).

Because biological transport is an important scientific problem, it seemed worthwhile to pursue the solute-solute interaction phenomena further. In vitro transport processes occur in biological systems that are heterogeneous in nature. While previous work on artificial membranes has attempted to dissect out the "solute drag" phenomena from a multitude of influences, the present work has attempted to add back at least some of these influences. In doing this, it is hoped that the relative importance of solute drag as a biological mechanism of solute

movement can be more accurately ascertained.

Perhaps the event that has the most influence on the passive movement of a solute, either across a membrane or through a solution, is the movement of the solvent. As far back as the early 1950's, workers have noticed this effect (25, 26, 27). Termed solvent drag, it has been documented in frog skin (27), toad bladder (28), mammalian intestine (29, 30, 31) and synthetic membranes (32), to name a few. Solvent drag is an especially important consideration when dealing with hypertonic solutions, because one must deal with the osmotic water flow generated by that solution. Workers studying the "apparent active transport" phenomena on frog or toad skin or toad bladder noted this osmotic water movement but did nothing to compensate for it. The net flows of solute in the inward direction were noted despite a net flow of water in the opposite direction. For simplicity, studies on artificial membranes were done with the water flow abolished by hydrostatic pressure.

The studies in this thesis add back the water flow to the artificial membrane system and attempt to quantitate its effect as compared to the solute-solute interaction effect. Synthetic membranes were chosen over biological membranes because synthetic membranes can withstand the pressure differences required to manipulate the osmotic water flow. It is hoped that these studies will further present knowledge of passive mechanisms of solute diffusion in synthetic and biological membranes.

Introduction to Membrane Transport

Every living cell is enclosed in a membrane that serves not only as a sturdy envelope inside which the cell can function but also as

a discriminating barrier, enabling nutrients and other essential agents to enter and waste products to leave. This organ, called the plasma membrane, is able to "pump" substances from one side of the membrane, where the concentration of that substance may be low, to the other side, where the concentration may be many times higher. By selectively regulating the flow of nutrients and ions, the plasma membrane is able to precisely maintain the cells internal milieu. The importance of this structure to the life process cannot be overstated.

Just as a plasma membrane encloses cellular protoplasm, epithelial membranes enclose, divide, and in other ways compartmentalize structures in multicellular organisms. In many respects the functioning of this higher order of membranes is analogous to the functioning of plasma membranes. Epithelial membranes, just as plasma membranes, are involved in transport of ions and nutrients from one compartment to an adjacent one. Further, these membranes regulate the flow of substances between compartments so as to maintain the desired distribution of solutes throughout the organism. The study of these transport properties of epithelia is both interesting and important and has been the concern of several scientific disciplines for many years.

The movement of substances across biological membranes, epithelial or cellular, is thought to occur by three different routes, namely: 1) direct passage of the substance through the lipo-protein matrix, either by dissolving in the lipid component of the membrane (33) or by being transported by a membrane protein (36); 2) engulfment of the substance by a process of vesiculation called pinocytosis (34, 35); or

3) penetration of the substance through pores (21, 37).

Of all these pathways the most is known about the later mechanism. In fact, investigators generally try to describe a transport process by pore theory first. Well worked out laws of permeation through pores are applied, and if theory doesn't match observation, the process is called anomolous and attributed to the first or second possibilities, of which less is known. For example, in many animals animo acids are transported from the gastrointestinal tract into the bloodstream against a concentration gradient (38). This observation clearly is anomolous in terms of simple diffusion and has been ascribed to specific energy dependent transport proteins in the mucosal cell membranes. Urea and mannitol, on the other hand, are examples of solutes whose movement across the intestine can, in general, be explained in terms of diffusion through pores (39, 40). In this case, it has not been necessary to consider a major involvement of either active transport or pinocytosis.

Theories describing diffusion through pores are far from simple, however,as several factors must be taken into account. Besides the concentration gradient for the substance, one must be aware of pressure gradients, solvent flows and flows of other substances. Failing to appreciate all the determinants of diffusion can lead to a gross misunderstanding of the mechanism of transport of a specific molecule. After a brief consideration of the anatomical sites of pores in epithelial membranes, this thesis will consider some common theoretical treatments of diffusion of substances through membrane pores.

Epithelial Structure Pertinant to Molecular Transport Through Pores.

Although epithelial membranes can contain many cell layers,

evidence indicates that in most cases one cell layer will be rate limiting for diffusion (41). Therefore, it is appropriate to talk of an epithelial membrane as being composed of a single sheet of cells. Electron microscopy shows that epithelial cells are linked together by cell to cell junctional structures at the apical regions of the lateral cell membranes (42,43). Jared Diamond's now classical "beer can model of epithelia" is helpful in understanding this structure. (44)

Consider a six pack of beer; each beer can represents a barrel shaped epithelial cell, the pop-top end corresponds to the apical cell membrane, the bottom to the basal cell membrane and the sides to the lateral cell membranes. The spaces between cans are the lateral intercellular spaces and the plastic which holds the cans together represents the tight junction (zonula occludens) of the junctional complex. The apical surface (the pop-top end) faces the lumen of an epithelial lined cavity in vivo while the basal surface (beer can bottoms) faces the blood stream in vivo. The tight junctions acts as a gate, regulating solute movement from the luminal solution directly into the lateral intercellular spaces. This regulation is largely a consequence of steric or structural hinderence, with the structure of the tight junction determining how large a molecule will be able to pass (45). Since the lateral intercellular spaces offer little resistance to diffusion of even large molecules, the structure of the junction determines the overal selectivity of the epithelia (45). It is these junctions that are thought to be analogous to the "pores" of synthetic membranes.

Theory : Fick's First Law of Diffusion

As with gases, the molecules that make up a solution are constantly in motion. This random movement tends to evenly dispense the molecules throughout the solution (48, 49, 50). At equilibrium the activity of any solute will be the same in all parts of the solution. A departure from this condition will lead to a net movement of solute from a region of high activity to one of lower activity. This net movement is described by Fick's first law (46) in which the flux of solute i is related to its concentration gradient, dc/dx, by the diffusion coefficient D:

$$J_{Di} = -D\ (dc/dx)i \qquad (1)$$

Application of this law to diffusion through a pourous membrane involves considering the concentration gradient for a solute that exists inside the membrane matrix. In the case where a membrane separates two solutions of unequal concentration it is thought that there will be linear concentration profile in the membrane's porous matrix, assuming the solute is small enough to permeate the pores and assuming the system is in a steady state condition (47). In this case the concentration gradient is just the difference in concentration of the two solutions divided by the membrane thickness, H. Restating Fick's law with this information gives:

$$J_{Di} = -D\ \Delta C/H$$

The J_{Di} in this equation refers to the rate of flow of solute i per unit area of open space. To define the rate of flow per unit membrane area, the fractional pore area Ap, must be introduced.

$$Ap = \frac{\text{total pore area}}{\text{total membrane area}}$$

and so,

$$J_{Di} = -D\ Ap\ \Delta C/H$$

Since Ap and H are often not known, they are incorporated along with the diffusion coefficient into a single term called the apparent permeability coefficient. Thus:

$$J_{Di} = -P \Delta C$$

Examination of the latter relation reveals that J_{Di}, the rate of diffusion of solute i through a membrane is dependent on two factors, ΔC and P. The concentration gradient term, ΔC, can be thought of as the force which causes solutes to diffuse across membranes. This term is actually an approximation of the thermodynamic driving force for diffusion, the transmembrane chemical potential difference for the solute. The other term, P, is a composite proportionality constant which takes into account properties of both the membrane and the solution. It can be thought of as the transmembrane flux of a solute at unit concentration difference.

Clearly, this simple relation does not reveal everything there is to know about a membrane-solvent-solute system. For instance, it does not reveal anything about the movement of the solvent. For this, a separate relation must be used; this is considered in the following section.

Osmotic Pressure.

Where a solution is separated from the solvent by a semipermeable membrane (permeable to solvent but not solute), the solvent flows through the membrane into the solution, where the chemical potential of solvent is lower. This process is known as osmosis. This flow of solvent through the membrane can be prevented by applying a sufficiently high pressure to the solution. The osmotic pressure, π, is the pressure difference across the membrane required to prevent spontaneous flow in

either direction across the membrane.

Vant Hoff, analyzing data on osmotic pressure of sugar solutions, found empirically that an equation analogous to the ideal gas law gave approximately the behavior of dilute solutions (51). This equation, now called vant Hoff's Law is:

$$\pi\overline{V} = RT \qquad (3)$$

where $\overline{V}$ is the volume of solution containing a mole of solute, R is the ideal gas contstant and T is the absolute temperature.

Knowing that, $\overline{V} = \frac{1}{C}$ where C = concentration per unit volume , a more useful form of the equation is:

$$\pi = \Delta C\ RT$$

where, ΔC = difference in solute concentration between the two solutions bathing the membrane.

This equation is only true if the membrane is perfectly semipermeable, that is, if it is impermeable to the solute, but permeable to the solvent. If the membrane is not perfectly semipermeable, the osmotic pressure will be lower than that predicted from vant Hoff's equation. Since most biological membranes are not perfectly semipermeable, a coefficient was added to vant Hoff's equation by Staverman (52). This factor is called the Staverman reflection coefficient, σ, and is equal to the observed osmotic pressure divided by the predicted osmotic pressure. Vant Hoff's equation now becomes:

$$\pi = \sigma\ \Delta C\ RT \qquad (4)$$

The meaning of σ is apparent from this equation. When $\sigma = 1$ the membrane is not permeable to the osmotic solute and the measured osmotic pressure is equal to that predicted by vant Hoff's original

equation. When σ is less than 1, however, some solute penetrates the membrane and the observed osmotic pressure is less than the theoretical one. When $\sigma = 0$ there is no osmotic pressure created by the solute because the membrane does not distinguish between the solvent and solute.

Thermodynamic Considerations

This section will discuss the use of thermodynamic formalism in the description of membrane transport processes. Since biological phenomena involving membranes, such as the transport of matter, are non-equilibrium, irreversible processes, the laws of classical thermodynamics are of limited usefulness. At best, these laws provide a set of inequalities describing only the direction of change. A more intellectually satisfying way to describe membrane phenomena is through the use of kinetic equations that are based on specific models. The construction of such models has contributed substantially to the understanding and visualization of many biological processes. Often, however, the development of an adequate kinetic description of the phenomena requires more detailed information than is available or readily obtainable. Indeed, this is often the case for membrane transport. An ideal method for describing biological phenomena would be one that is independent of specific kinetic or statistical models, yet would still enable a quantitative description of irreversible processes. A relatively new field, the study of irreversible thermodynamics, attempts to formulate such a method.

A starting point for the application of irreversible thermodynamics to membrane transport phenomena is the "dissipation function". The dissipation function describes the rate of energy dissipation or

internal entropy production in a system which is not at equilibrium but approaches equilibrium. In a system involving membrane transport this dissipation function equals the product of a given flow and its' conjugate driving force, where the conjugate driving force is the difference in chemical potential across the membrane for that species (53). In other words, the dissipation function is the rate at which the energy inherent in a chemical potential difference is dissipated by the flow of conjugate species down that potential difference. So, for a membrane system at constant temperature:

$$\Phi = (ds/dt)_T = \sum_i^n J_i \, \Delta\mu_i \qquad (5)$$

where Φ represents the dissipation function for the membrane, J_i represents the flux of the ith component across the membrane and $\Delta\mu_i$ represents the difference in chemical potential across the membrane for component i. For a binary solution of nonelectrolytes across a simple membrane this expands to:

$$\Phi = J_s \, \Delta\mu_s + J_w \, \Delta\mu_w \qquad (6)$$

where the subscripts s and w refer to, respectively, the solute and the solvent.

A problem with the above equation is that the quantities involved are difficult to determine experimentally. Kedem and Katchalsky (54), have transformed this equation into one which the variables are readily measureable in most membrane systems. The transformation involves the explicit expressions of the chemical potentials μ_s and μ_w:

$$\Delta\mu_w = \overline{V}_w \, (\Delta P - \Delta\pi) \text{ and,} \qquad (7)$$

$$\Delta\mu_s = \overline{V}_s \, \Delta P + \Delta\pi/\overline{C}_s \qquad (8)$$

where, $$\bar{C}_s \approx \frac{C_1 + C_2}{2} \qquad (8a)$$

C_1 and C_2 equal the concentrations of solute on either side of the membrane.

Inserting these expressions into equation 5, it can be shown (54) that the dissipation function becomes:

$$\Phi = \Delta P\, J_v + \Delta\pi\, J_D \qquad (9)$$

where, J_v = the total volume flow (solvent and solute) across the membrane and, J_D = the flow of solute relative to the flow of the solvent. In this transformed equation the new conjugate forces are the difference in hydrostatic pressure ΔP and the difference in osmotic pressure $\Delta\pi$ across the membrane.

The next step is to relate these new forces to their conjugate flows, J_v and J_D, by a set of phenomenological equations. It is empirically known that if the force driving a flow across a barrier is small, the flow is linearly related to the driving force so that,

$$Ji = Lii\ Xi$$

where Ji is the transmembrane flow of species i, Xi is the force driving the flow of i and Lii is the flow of i per unit driving force. In a system that contains more than one flow, each flow may be influenced by every other flow and hence by forces other than its conjugate force. A set of phenomenological equations describing the flows of solutes i through n for such a system are as follows:

$$\begin{aligned} Ji &= Lii\ Xi + Lij\ Xj + Lik\ Xi \ldots Lin\ Xn \\ Jj &= Lji\ Xi + Ljj\ Xj + Ljk\ Xk \ldots Ljn\ Xn \\ Jn &= Lni\ Xi + Lnj\ Xj + Lnk\ Xk \ldots Lnn\ Xn \end{aligned} \qquad (10)$$

For the two component systems represented by equation 9, the phenomenological equations are thus :

$$J_v = L_P \Delta P + L_{pD} \Delta\pi \qquad (11)$$

$$J_D = L_{DP} \Delta P + L_D \Delta\pi$$

Some common physical situations will serve to clarify the significance of these equations. First, consider the situation in which the concentration of the solute is the same in both membrane bathing chambers. In this case $\Delta\pi$ equals zero and only the first terms remain in the equations. When a hydrostatic pressure difference is created, a volume flow through the membrane will occur. Equation 11 states that the magnitude of the volume flow will be linearly related to the hydrostatic pressure difference by the hydraulic conductivity, L_p. Equation 12 predicts the possibility of a movement of solute relative to solvent, J_D, as additional effects of a hydrostatic pressure difference. This phenomena is called ultrafiltration and L_{PD} is sometimes called the coefficient of ultrafiltration.

Now imagine the situation in which the hydrostatic pressure difference is zero and an osmotic pressure gradient is created by having different concentrations os the solute in the membrane bathing solutions. In this case, the first terms will drop out in equations 11 and 12. The diffusional flow of solute caused by its concentration gradient is described by the coefficient L_D in equation 12. Examination of equation 11 shows an addition effect, a volume flow caused by an osmotic

pressure difference in the absense of a hydrostatic pressure difference. This well known phenomena is the osmotic flow and L_{PD} is readily identified as the coefficient of osmotic flow.

Onsager (55) demonstrated in 1931 that for linear phenomenological equations, such as equation 10, 11, and 12, the reciprocal cross term coefficients are equal. Considering the generalized equation, 10, this means that Lix = Lxi for all x. The significance of this observation can be more readily understood by examination of equations 11 and 12. In this case, Onsanger's reciprocal relation maintains the cross term constants L_{DP} and L_{PD} are equal, indicating that the volume flow per unit osmotic pressure should be equal to the diffusional flow per unit pressure difference. This equality is reasonable considering both phenomena depend on the selectivity of the membrane for solvent over solute.

Staverman (52, 56), realizing the need for a measure of membrane selectivity, developed what is called the Staverman reflection coefficient, σ. To understand how this value works, consider the experiment in which solutions on both sides of a membrane contain equal concentrations of solute. Equations 11 and 12 reduce to:

$$(J_v)_{\Delta\pi=0} = L_P \Delta P \tag{13}$$

$$(J_D)_{\Delta\pi=0} = L_{DP} \Delta P \tag{14}$$

First, imagine a membrane that has very large pores in relation to the molecular size of the solute, so large, in fact, that when a pressure difference forces the solution of one side across the membrane, the solute flow is not restricted with respect to the solvent flow ($J_D = 0$). In this case,

there is no ultrafiltration and L_{DP} equals zero. Now imagine the other extreme, where the membrane is so selective (has such small pores) that no solute crosses no matter how large the solvent flux. In this second case, there is no flux of the solute, so J_v and J_D must both reflect the movement of the solvent. The values of J_v and J_D, therefore, are equal in magnitude but opposite in sign because the movement is, with J_v, with respect to the membrane and with J_D, with respect to the solute (which is stationary). Then, since J_v equals $-J_D$, L_{DP} will equal $-L_P$.

One can see, therefore, that the value of L_{DP} varies from zero to $-L_P$ depending on the selectivity of the membrane, and, further, that the value of $\frac{-L_{DP}}{L_P}$ will vary between zero and one. Staverman defined this number as the reflection coefficient:

$$\sigma = \frac{-L_{DP}}{L_P} \tag{15}$$

A nonselective membrane will have a reflection coefficient close to zero and a relatively selective membrane will have a reflection coefficient close to one.

Using the above equations and definitions one can derive other equations that are helpful for understanding membrane transport processes. For instance, introduction of σ into equation 11 (remember $L_{DP} = L_{PD}$) gives,

$$J_v = L_P (\Delta P - \sigma \Delta \pi) \tag{16}$$

This equation shows how hydrostatic and osmotic pressures additively combine to produce a volume flow.

It is sometimes helpful to study the total solute flow, J_s, rather than the relative solute flow J_D. It can be shown that, (57)

$$\frac{J_s}{\overline{C}_s} = J_v + J_D \tag{17}$$

where $\overline{C}_s$ was defined in equation 8a. Introducting equations 11 and 12, the equation becomes,

$$\frac{J_s}{\overline{C}_s} = (L_p + L_{DP})\ \Delta P + (L_{PD} + L_D)\Delta\pi \tag{18}$$

Solving equation 16 for ΔP and substituting this into equation 18, then using the definition of σ and keeping in mind Onsager's reciprocal relation one can derive the following:

$$J_s = \overline{C}_s\ (1 - \sigma)\ J_v + \omega\Delta\pi \tag{19}$$

where, $\omega = \dfrac{\overline{C}_s\ (L_P L_D - L_{PD}^{\,2})}{L_P}$

The new coefficient, ω, is the coefficient of solute permeability at zero volume, and is an important characteristic parameter of both biological and synthetic membranes.

The significance of equation 19 can be grapsed by considering that in a solute system the flow of that solute across the membrane is the result of either: 1) diffusion down a concentration gradient, or, (2) solvent drag as a result of volume flow, J_v.

The former is reflected by the $\omega\Delta\pi$ term. In the absense of a volume flow equation 19 reduces to:

$$J_s = \omega\Delta\pi$$

This term might be more easily understood by substituting ΔC, the concentration difference for the solute, for $\Delta\pi$. To do this, use the relation $\Delta\pi = RT\Delta C$ and define $P_s = \omega RT$. The expression then becomes:

$$J_s = P_s \Delta C$$

This new expression is similar to Fick's first law of diffusion as applied to membranes. The difference is that P_s (above) relates solute permeability at zero volume flow, whereas this condition is not required for the P in Fick's law. Also, P_s equals -P from Fick's law.

The latter is reflected by the $\overline{C}_s (1 - \sigma) Jv$ term. When the concentration of solute is equal on both sides of a membrane equation 19 reduces to:

$$J_s = \overline{C}_s (1 - \sigma) J_v$$

This is the solvent drag term. It states that the amount of solute dragged is directly related to both the average concentration of solute, $\overline{C}_s$, and the rate of volume flow, J_v. The proportionality constant is the value of $(1 - \sigma)$. One can see that as the membrane gets more selective, i.e., as σ approaches 1, more solute will be reflected, leading to a decrease in the solvent drag term.

Extension of the Theory to a Two Solute System.

Equation 19 is applicable to a situation in which one solute diffuses and/or is dragged by solvent through pores in a membrane. What if a second solute is added? How does this second solute effect the flow of the first solute? From now on the first solute will be referred to as the tracer since it is the solute whose flow is to be followed.

One effect the addition on a second solute has on the flow of a tracer solute is to slow the free solution diffusion of the tracer.

This occurs because of an increase in the "viscosity" of the solution. On a molecular level this can be envisioned by the idea that the rate of movement of the tracer through the solvent is restricted by collisions with the second solute. The magnitude of this effect is determined by the molecular dimensions and concentration of the second solute.

A second effect an additional solute might have on the flow of a tracer solute is related to the movement of the solvent. If there is an osmotic pressure gradient for the second solute, this will create a volume flow, J_v, that might drag some tracer. The magnitude of this effect will be related to the rate of the volume flow and the size of the tracer in relation to the membrane pore diameter. An osmotic pressure difference for the second solute will have an effect on volume movement that adds to the effect of any hydrostatic pressure differences, as shown by equation 16.

Neither of these first two effects of an additional solute, increased solution viscosity nor changed volume flows, necessitate changes in equation 19. The first effect, increased viscosity, will manifest itself in an altered coefficient of solute permeability, ω. Usually the second solute will decrease the value of ω, indicating that the membrane has become less "permeable". The second effect, changed volume flow, will effect tracer flow in a way already described by the term $\bar{C}_s (1 - \sigma) J_v$. In essence, the second solute has created a volume flow that participates in a solvent drag effect. This solvent drag effect is exactly analogous to the effect produced by volume flows that are the result of hydrostatic pressure differences.

A third effect of a second solute is not covered by equation

19. This effect comes into play if there happens to be a flow across the membrane of the second solute. In this case there might be a direct interaction between the two solutes such that the flow of the second solute will influence the flow of the tracer solute.

Van Bruggen and coworkers (23) have realized that interaction of solute flows is qualitatively similar to the effect of solvent drag as presented in equation 19. In both cases the effect on tracer flow is proportional to: 1) the concentration of the tracer, $\bar{C}_s$, 2) the magnitude of the driving force, J_v in the case of solvent drag and J_D[1] in the case of interacting solute flows, and 3) a proportionality constant, $(1-\sigma)$ in the case of solvent drag and a new constant, λ, in the case of interacting solute flows. In light of these similarities an expression describing solute-solute flow coupling was developed:

$$\begin{matrix}\text{net tracer flow resulting} \\ \text{from solute-solute interaction}\end{matrix} = \bar{C}_s \lambda J_D \qquad (20)$$

where, λ = the coefficient of interaction between the two solutes.

With this relation, Kedem and Katchalsky's equation (equation 19) can be expanded to cover a two solute system. Assuming the solute drag effects are independent and additive,

$$J_s = \omega\Delta\pi + \bar{C}_s (1 - \sigma) J_v + \bar{C}_s \lambda J_D \qquad (21)$$

This equation states that the flow of a tracer, J_s, in a two solute system can be broken down into three components, each represented by a term in equation 21, and each term being independent of any other term. A generalized form of equation 21 is:

---

[1] The second solute will often be referred to as the driver. The transmembrane flow of this solute is denoted as J_D.

$$J_s = J_{\text{Diffusion}} + J_{\text{solvent drag}} + J_{\text{solute drag}} \quad (22)$$

Membranes

The experiments described here were carried out on synthetic membranes of two types : a homoporous polycarbonate membrane, and three heteroporous cellulose membranes. A number of physical characteristics of these membranes are listed in table I.

The homoporous polycarbonate membrane, on which the first studies were carried out, was manufactured by Nucleopore Corporation, Pleasanton, Calif. At the time this membrane was obtained, Nucleopore did not have a commercially available membrane with pores small enough for our laboratory's purposes. The particular piece utilized in this study was an experimental piece kindly supplied to our labratory by Nucleopore. This membrane's manufacture was by a process similar to the manufacturing process of all Nucleopore membranes. This process (58→61) involves irradiation of polycarbonate films by fission fragments which drill "damage tracks" in the material. Etching of the damage tracks with NaOH under controlled conditions of temperature and in the presence of wetting agents provides a membrane with pores of measureable size and abundance. These pores are considered to be essentially at right angles, but a maximum deviation of 20° from the right angle may be present.

The homopore membrane showed in a hydraulic conductivity coefficient of 0.90×10^{-10} $cm^3 dyne^{-1} sec^{-1}$ The experiment to determine this value is reported later in this thesis. The effective pore radius calculated from the method of Goldstein and Solomon (21) gave a value of 180 Å. Another method of estimating the effective pore radius depends on the diffusive permeability of water as compared to the

Table I

Characteristics of Synthetic Membranes

		Nucleopore 86	S and S RC52	S and S AC62	S and S RC51
1. Structure		polycarbonate	cellulose acetate	cellulose acetate	cellulose acetate
2. Thickness		6	100	90	90
3. L_p cm^3 $dyne^{-1}$ sec^{-1}		0.90×10^{-10}	1.45×10^{-10}	1.89×10^{-10}	0.59×10^{-10}
4. P_{H_2O}		1.00×10^{-4}	6.52×10^{-4}	4.51×10^{-4}	9.70×10^{-4}
5. Reflection coefficient* for sucrose		0.020	0.043	0.031	0.080
6. Effective pore radius A	a.**	180	100	120	55
	b. +	130	70	90	35

* Determined by comparing theoretical and experimental osmotic pressure.

** By method of Goldstein and Solomon. (21)

\+ By method of Pappheimer et al (62)

hydraulic conductivity, L_p. This method, developed by Pappenheimer et al (62) gives a value of 130 Å. These methods will be discussed in more detail later in this section.

The second type of synthetic membrane used was the cellulose acetate membrane filter commercially available from Carl Schleicher and Schuell Company, Keene, New Hampshire. Three different membranes were used, numbers RC 52 RC51 and AC62 as labelled by the company. The manufacturer states that these filters "have an extremely uniform micropore structure and are approximately 100 Å, thick." The advertised effective pore radii are 50 to 100 Å for RC 52 and AC62, and less than 50 Å for the RC 51 membrane. Riley et al (63) have shown by electron microscopy that cellulose acetate membranes have an extremely thin and dense surface skin overlying a much more porous and thick backing. It is felt that the dense skin layer is responsible for the filtration properties of the membrane while the porous backing offers little resistance to flow . Despite the asymmetrical structure, asymmetrical diffusive permeabilities for tracer water were not observed under the conditions of our studies.

The relevant data for these membranes is presented in table I. Note that, as claimed by the manufacturer, the RC51 has smaller pores than either the RC52 or AC62 membranes. In addition, the RC52 appears to have slightly smaller pores than the AC62, however, this difference may not be significant considering the accuracy of the methods involved.

Solutes

Solutes used in this work were sucrose, urea, mannitol, raffinose and polyelylene glycol 600. Table II represents a

Table II

Molecular Dimensions of Solutes

		Molecular radius Å			
Solute	Molecular Weight	Diffusion experiments	References	Viscosity experiments	References
DHO	19	1.9	(75)		
urea	60	2.7	(75)		
mannitol	182	4.4	(75)	3.8	(62)
sucrose	342	5.3	(75)	5.0	(62)
raffinose	504	6.1	(75)	5.7	(62)
PEG 600	570-630			7.7	(76)

compilation of molecular dimensions for these solutes found in the literature.

Reagent grade urea, sucrose and raffinose were obtained from J.T. Baker Chemical Company, Phillipsburg, N.J., as was polyethelene glycol 600. The polyethelene glycol was stated by the manufacturer to have an average molecular weight of between 570 and 630, an apparent specific gravity at 20 degrees of 1.1279 and complete solubility in water at 20 degrees. The mannitol was obtained from Mallinckrodt Chemical Works, St. Louis, Missouri. These compounds were used as hyperosmotic agents.

Radioactively labelled sucrose [^{14}C(U)] and raffinose [^{3}H(G)] were obtained from New England Nuclear Corporation, Boston, Mass. Tracer mannitol [1-^{14}C] was obtained from Amersham Corporation, Arlington Heights, Illinois. These compounds were dissolved in distilled and micro-filtered water to a known volume before being used as molecular probes in experiments. Tritiated water for determining the diffusive permeability of solvent was obtained from New England Nuclear Corporation.

The solvent in all experiments was water,treated in each case by distillation and filtration through 0.05 μ Nucleopore membranes. Care was taken in the preparation of solutions to avoid contamination by dust or other foreign substances. This was considered especially important as the clogging of membrane pores by foreign particles could substantially alter permeability results.

Measurement of Solute Fluxes

Many of the experiments carried out consisted of the measurement of a flux of a tracer solute across a membrane. The general

procedure for such experiments is as follows. On one side of the membrane is placed a solution containing the radioactive tracer solute. To this is added unlabelled solute of the same compound to make the solution one millimolal for the solute. The opposite solution is also made one millimolal with the nonradioactive solute. After an initial equilibration period to allow the development of a steady state, an aliquot of the formerly non-radioactive solute is taken by micropipette or syringe and an equal volume of non-labelled solution is replaced so that the volume of the solution remains constant. Samples are taken continuously in this way, at regular intervals, usually ten minutes, for five consecutive periods.

The permeability coefficients of solutes are determined by dividing the amount of radioactive tracer moving across a unit area of membrane in an interval of time by the concentration of the radioactive tracer in the donor solution. Hence P is a rate constant with dimensions of cm per second. The equation used is:

$$P = \frac{\Delta A}{t \quad Ma \quad Ad} \qquad (22)$$

where, t equals the time elapsed during the sample interval; Ma equals the area of the membrane (8 cm^2 in most cases); Ad equals the activity in disintegrations per minute per gram of H_2O in the donor solution; and ΔA equals the change in the activity of the solution from which the sample is taken. ΔA is calculated by the following equation:

$$\Delta A = \frac{(\text{DPM at time 1})\ (\text{volume of receiver chamber})}{(\text{sample volume at time 1})} -$$

$$\frac{(\text{DPM at time 0})\ \left[(\text{volume of receiver chamber}) - (\text{time 0 sample volume})\right]}{(\text{sample volume at time 0})}$$

The radioactivity of the solutions were determined by liquid scintillation spectroscopy on a Packard Tri-Carb liquid scintillation spectrometer. The sample to be assayed was added directly to 10 ml of scintillation fluid in glass vials made by the Kimble Company of Toledo, Ohio. The scintillation cocktail consisted of 95% Aquasol (New England Nuclear, Boston, Mass.) and 5% water. The purpose of the water was to aid in the dispersion of the samples.

In this thesis unidirectional permeability coefficients are sometimes used to calculate net solute fluxes. This can be done when the left-to-right and right-to-left P values for a single solute under identical conditions are known. The relation used for this calculation is:

$$\overline{C}_s \, (P_{R \to L} - P_{L \to R}) = J_s \qquad (23)$$

Apparatus

The apparatus in which the experiments were carried out is diagrammed in figure 1. Each membrane was mounted in a stainless steel cassette whose structure is also shown in figure 1. The seal between the membrane and the cassette is provided by gaskets made of medical grade silicone rubber. The 20 mesh screen furnishes support for the membrane yet offers negligible restriction to diffusion. The membrane containing cassette is positioned between two plastic chambers, each with ports for filling, draining, and pressure or flow monitoring. The filling ports are sealed with diposable rubber closures, Criptocaps J (Clay-Adams Inc. New York, N.Y.), and the closures are held in place by hollow threaded plastic plugs. Through the

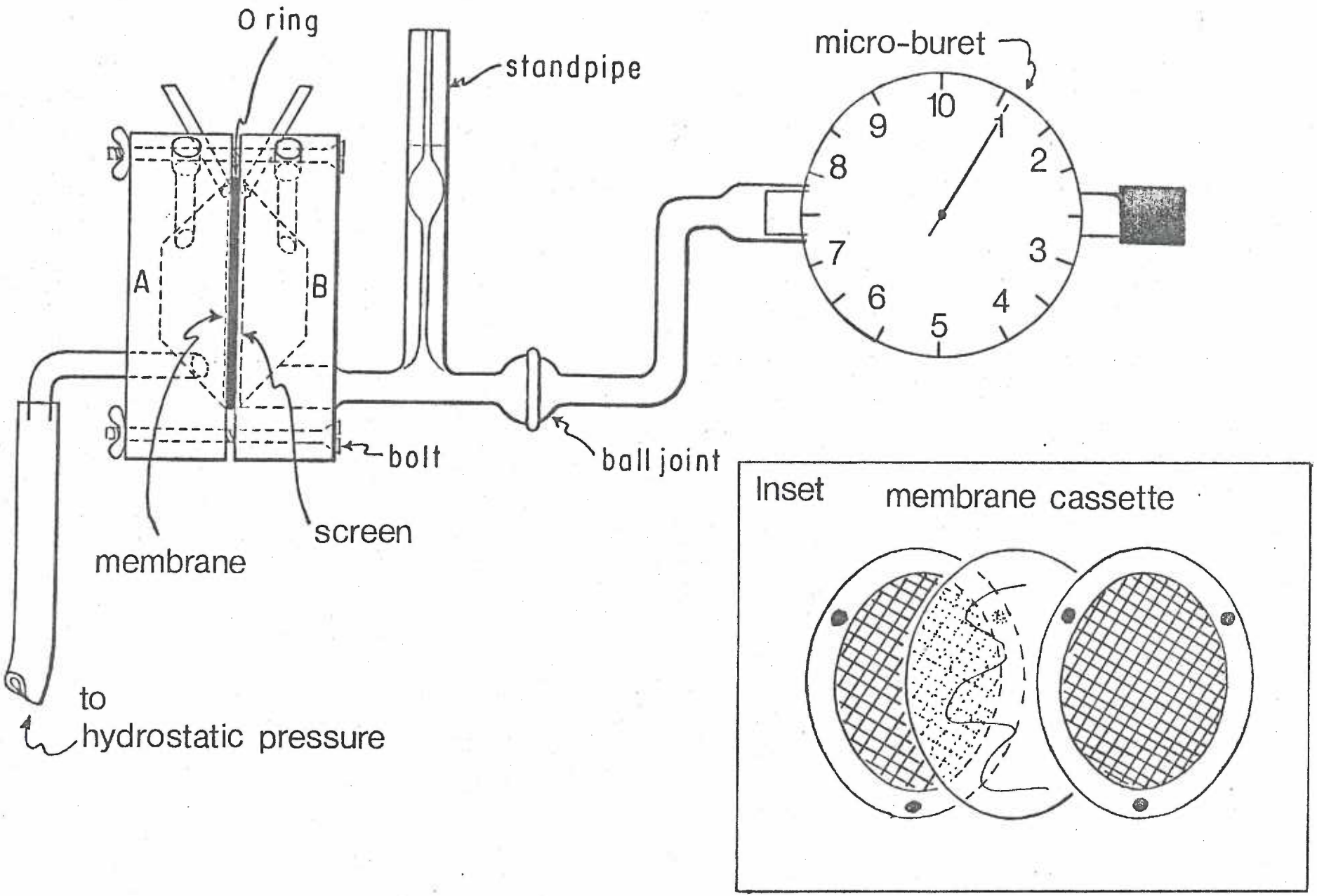
O ring
standpipe
micro-buret
A
B
bolt
ball joint
membrane
screen
to
hydrostatic pressure
Inset
membrane cassette

hollow plug can be inserted a syringe needle, with a medal stopcock (Becton, Dickerson and Co., Rutherford, N.J.) and syringe attached, allowing for sampling of the chamber contents or adding more solution. The drain ports in the bottom of the chamber are sealed by metal stopcocks as are the other two ports toward the front of the chamber. Inside each chamber is placed a small Teflon coated magnetic stir bar. These stirrers are driven by external magnets mounted on 600 rpm synchronous clock motors available from Herbach and Rademon, Philadelphia, Penn. The system is closed by wingnut applied pressure, the seal between the stainless steel cassette and the chambers being made by Neoprene O-rings embedded in the faces of the chambers.

Stopcocks on either side of the chamber can be attached to a pressure device. In the device used for these studies, pressure is attained by pumping air into a mercury reservoir by a hand-operated bulb and the resultant pressure measured by a height of a column of mercury produced in a stand pipe attached to the reservoir. Fine adjustment of the pressure is made by the displacement of a screw driven plunger in the barrel of a 10 ml syringe. A tight air seal between the barrel and the plunger is made by a mercury reservoir seal fashioned at the top of the syringe barrel. With this device hydrostatic pressures of between 0 and 80 cm of Hg can be accurately measured and maintained. Usually, the stopcocked port toward the front of the left hand chamber was the recipient of the pressure. The corresponding port on the right hand chamber was used to monitor rates of volume flow.

Volume flow is measured with a micropipet-buret (Beckman

Scientific Instruments, Irvine, Calif.) which is attached to a glass capillary standpipe as shown in figure 1. The microburet has a total capacity of 1 ml and each revolution of the dial is equal to 1 ul. The standpipe has a reference mark above the reservoir bulb which corresponds to the top of the water level in the chamber. To measure a volume flow the plunger of the micro-buret is either advanced or retracted to bring the water meniscus in the standpipe to the reference mark. The amount of fluid added or removed from the system in order to maintain the level of the menisous in the standpipe is the net volume flow across the membrane and is read directly from the microburet. Volume flows can be measured whether they occur from hydrostatic or osmotic pressure. Precision of plus or minus 0.2 ul per min. was obtainable.

Pore size determinations

This study concerns itself with the effects of solvent flow on the movement of a tracer across a membrane, the solvent drag effect, and the interaction of two solutes, solute drag. Both of these effects are influenced by the size of the pores of the membrane in which the studies are being carried out. For solvent drag, this is clearly shown by the presence of σ, a measure of membrane selectivity, in the equation for tracer flux derived by Kedem and Katchalsky (see eq. 19). For solute drag, a relationship between solute interactions and pore size was demonstrated by Galey and Van Bruggen (17). Because of these relationships, it was felt that effective pore radii of the membranes to be investigated should be known. The two methods used to estimate

pore dimensions are described below. Results of the determinations are listed in Table I, columns six and seven.

If one knows the molecular radius of a substance and the reflection coefficient for that substance in a membrane, the effective pore radius of the membrane can be calculated by the method of Goldstein and Solomon (21). The equation:

$$1-\sigma = \frac{[2(a/r)^2 - (1-a/r)^4]\,[1-2.104\ a/r + 2.09(a/r)^3 - 0.95(a/r)^5]}{[2(1-aw/r)^2 - (1-aw/r)^4]\,[1-2.104\ aw/r + 2.09(aw/r)^3 - 0.95(aw/r)^5]} \quad (24)$$

where a equals the radius of the solute molecule, aw equals the radius of the water molecule, and r equals the equivalent pore radius is derived by Goldstein and Solomon from the equation of Renkin (64). Using this equation it is possible to generate a family of curves $(1-\sigma)$ as a function of the permeant molcular radius. Each curve represents a single equivalent pore radius. Finding the curve that corresponds to experimentally determined reflection coefficients allows an estimation of membrane pore dimensions. See figure 2.

A second method involves comparing the diffusive flow of water across a membrane to the viscous flow of water across the same membrane. This method of determining the effective pore radius, which has been used by a number of investigators (22, 64, 65, 66) was initially developed by Pappenheimer et al. (62) and Koefoed-Johnsen and Ussing (37). The general equation used is:

$$r = \sqrt{\frac{8\eta\, D_{H_2O}\, L_p}{P'_{H_2O}}}$$

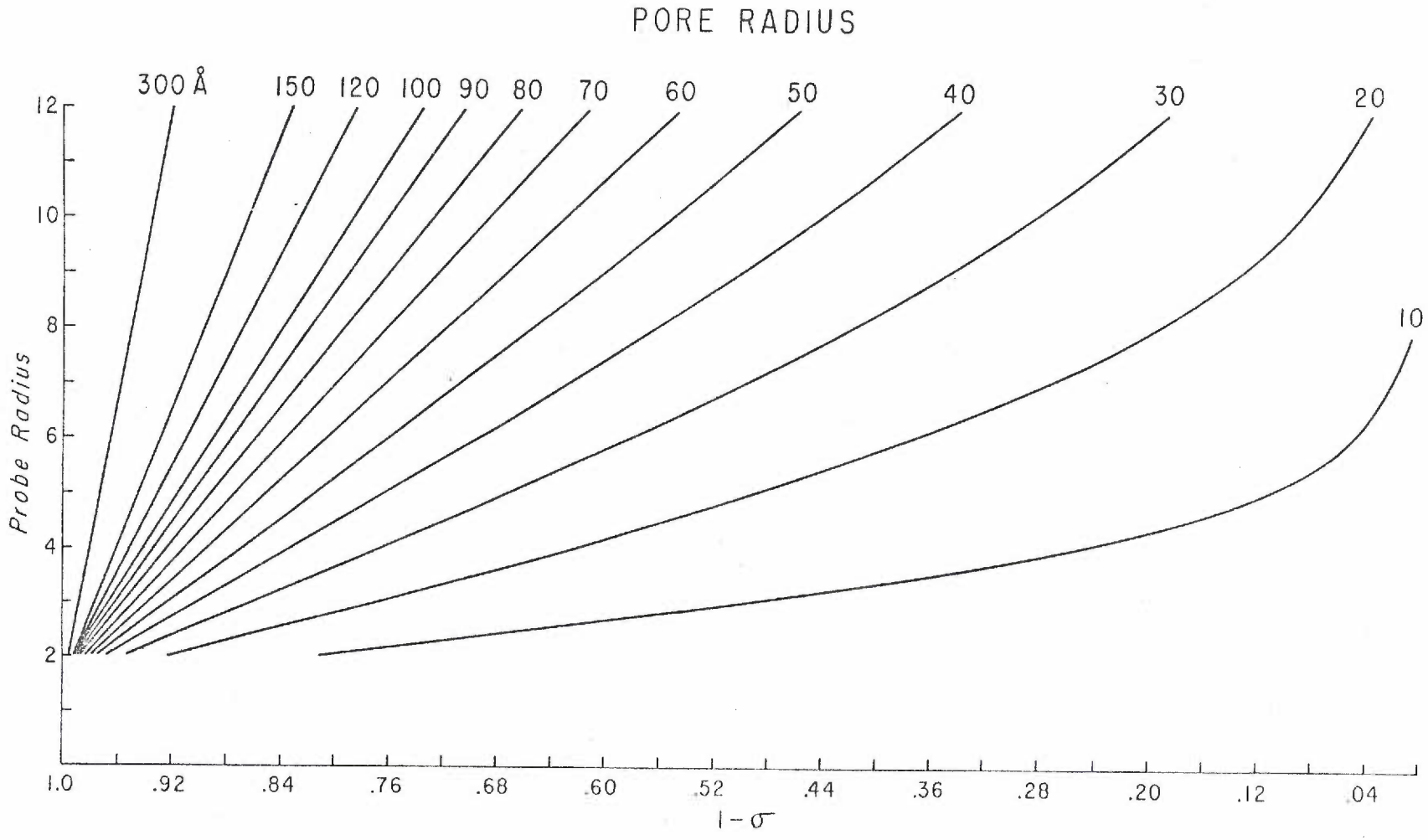
PORE RADIUS
300 Å
150
120
100
90
80
70
60
50
40
30
20
10
Probe Radius
12
10
8
6
4
2
1.0
.92
.84
.76
.68
.60
.52
.44
.36
.28
.20
.12
.04
1 − σ

where η equals the viscosity of water, D_{H_2O} equals the diffusion coefficient of water, L_p the hydraulic conductivity coefficient and P_{H_2O} the permeability coefficient for water.

Studies carried out in our laboratory (3, 4, 8, 17, 23), as well as those of others (1, 12, 24), have shown that asymmetrical solute fluxes across biological and synthetic membranes can be produced by a transmembrane flux of a second solute. This effect is thought to be due to frictional interaction between the solutes and has been termed solute drag. Studies reported by Ussing and Andersen (27), and others (67) and more recently by Froemter et al (68) and Ochsenfahrt and Winne (69, 70, 71) have shown that asymmetrical solute fluxes across a variety of biological membranes can be produced by a net flux of water in an effect termed solvent drag. This effect, too, is thought to be due to frictional interaction, this time between the solute and the solvent molecules. In vivo, it is likely that both solute and solvent drag contribute to the transmembrane flow of solutes. No study exists, however, that considers these two effects on solute movement simultaneously. Specific questions to be asked are: 1) Is one effect of such quantitative proportions as to render the other effect of little importance and, if not; 2) Are the two effects of an independent and additive nature as predicted by the theoretical equations? The experiments reported in this thesis were designed to answer these and other questions.

Since transmembrane water flow was to be such an integral part of the experimentation it seemed necessary to study this factor first in some detail. To begin with, experiments were done in which a hydrostatic pressure gradient was imposed across a Nucleopore membrane (no. 86) and the resultant flow measured. Theory predicts

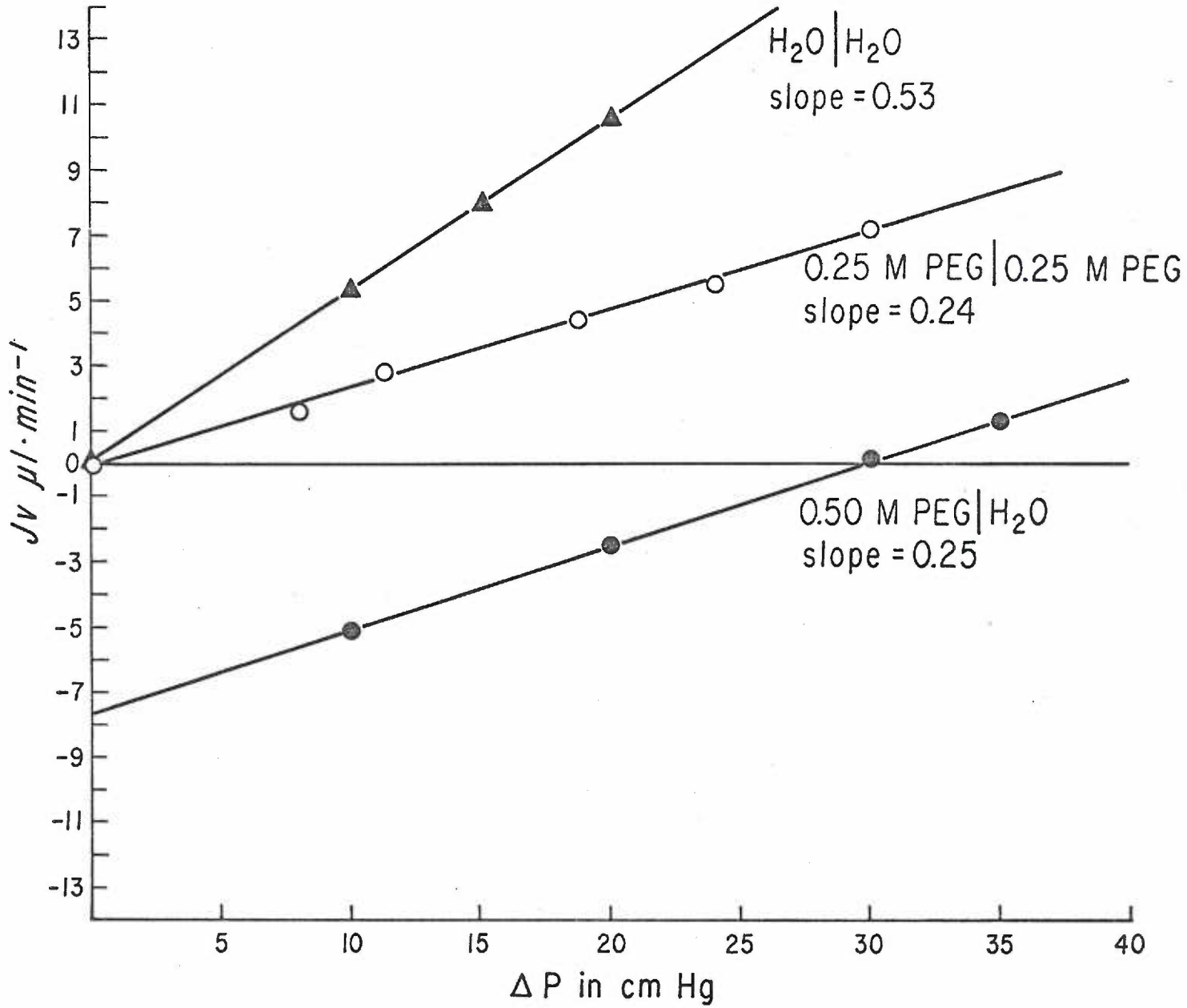
$H_2O|H_2O$
slope = 0.53
0.25 M PEG|0.25 M PEG
slope = 0.24
0.50 M PEG|H_2O
slope = 0.25
Jv μl · min⁻¹
ΔP in cm Hg
13
11
9
7
5
3
1
0
-1
-3
-5
-7
-9
-11
-13
5
10
15
20
25
30
35
40

that water flow will be linearly related to pressure, with the slope of the line from such an experiment being related* to the coefficient of hydraulic conductivity, L_p (47). The top line in figure 3 represents the results of this work. It can be seen that the slope equals 0.528 ul/min and that, as predicted, the relationship between pressure and flow is linear over the range measured.

Movement of liquid through membrane pores can be expected to obey Poiseuille's law, which states that the coefficient of hydraulic conductivity will be related to the number of pores in the membrane, the fourth power of the radius of the pores and inversely related to the viscosity of the solution in the pores. At a molecular level the term "viscosity" is confusing, so some authors replace this term with a more general one, pore environment. It is apparent that the coefficient L_p can be considered an indicator of the pore environment of any one membrane during different conditions. A lower L_p value means that the pore environment is such that more pressure is needed to cause a certain volume flow.

The middle line of figure 3 represents an experiment in which both of the solutions bathing the membrane were 0.25 molar PEG 600. The line is linear, and, as expected from Poiseuille's law, the slope is decreased from the situation in which water bathed the membrane. It can be said that because of the presense of the PEG, the pore environment is more restrictive, by about 50 percent, than in the case of pure water. It follows that as more solute is added to the solution the value of L_p thus the slope will decrease even further.

---

* volume flow needs to be expressed "per membrane area for the slope to equal L_p"

Volume flows across membranes can be generated by osmotic pressure as well as by hydrostatic pressure. Most workers in the field believe that these two types of pressure are of a similar molecular nature, both being bulk flow processes. Moreover, equations derived from irreversible thermodynamics state that osmotic pressure and hydrostatic pressure will influence volume flows in a manner which is additive. The pertinant equation is:

$$J_v = L_p (\Delta P - \Delta \pi_e) \qquad (26)$$

where $\Delta \pi_e$ is the experimentally measured osmotic pressure and the other symbols have their usual meaning.

The bottom line in figure 3 represents an experiment in which both hydrostatic and osmotic pressure differences are operative. PEG 600 at 0.681 molal concentration was placed on one side of the membrane and pure water on the other. The osmotic pressure generated by this condition is quantitated by the amount of hydrostatic pressure that is needed to block the induced flow. This value, $\Delta \pi$, is read from the graph at the point where the line intercepts the line of zero volume flow, at 30 cm. H_g in this case. As the hydrostatic pressure is gradually reduced from this point, the osmotic pressure difference causes a volume flow. This volume flow is at its' greatest when there is no hydrostatic pressure to counterbalance the osmotic pressure. For this system, a value of -7.7 ul per min can be read at the intercept of the ordinate.

Rearrangement of equation 26 into a slope-intercept form reveals that the slope of the bottom line in figure 3 is related to the L_p of the

experiment. It is important to note that the value of L_P in this case is similar to the value of L_P for the experiment represented by the middle line, in which .29 molal PEG bathed both sides of the membrane. This similarity of L_P values suggests a similarity of pore environments for these two experimental conditions. This is the basis for "P 1/2 C" experiments to be explained later.

As developed in the theoretical section of this thesis, the flux of a solute across a membrane can be broken down into three component flows, all due to different forces. The generalized equation presented was:

$$J_s = J_{s(C_s)} + J_{s(J_v)} + J_{s(J_D)}$$

where the three terms represent diffusion down a chemical potential gradient, solvent drag and solute drag, respective. As stated in the introduction, the focus of this thesis will be on the latter two component fluxes. To this end the next phase of the experimentation involved quantitation of the solvent drag component, $J_{s(J_v)}$.

Figure 4a shows unidirectional permeability coefficients for tracer sucrose across the Nucleopore 86 membrane as a function of volume flow. At zero volume flow, the tracer can be expected to diffuse across the membrane purely as a consequence of its chemical potential gradient. Therefore, the permeability coefficients for sucrose in the L→R and R→L directions should be equal. Note that this has been demonstrated to be the case at $J_v = 0$ in figure 4a. As the volume flow increases, the unidirectional permeabilities of tracer in the same direction as the volume flow increase while the unidirectional permeabilities in the

FIGURE 4

a. The effect of volume flow on unidirectional tracer sucrose permeabilities.

b. Net fluxes of sucrose as a function of volume flow. These values were calculated from those in figure 4a.

A Nucleopore 86 membrane was used.

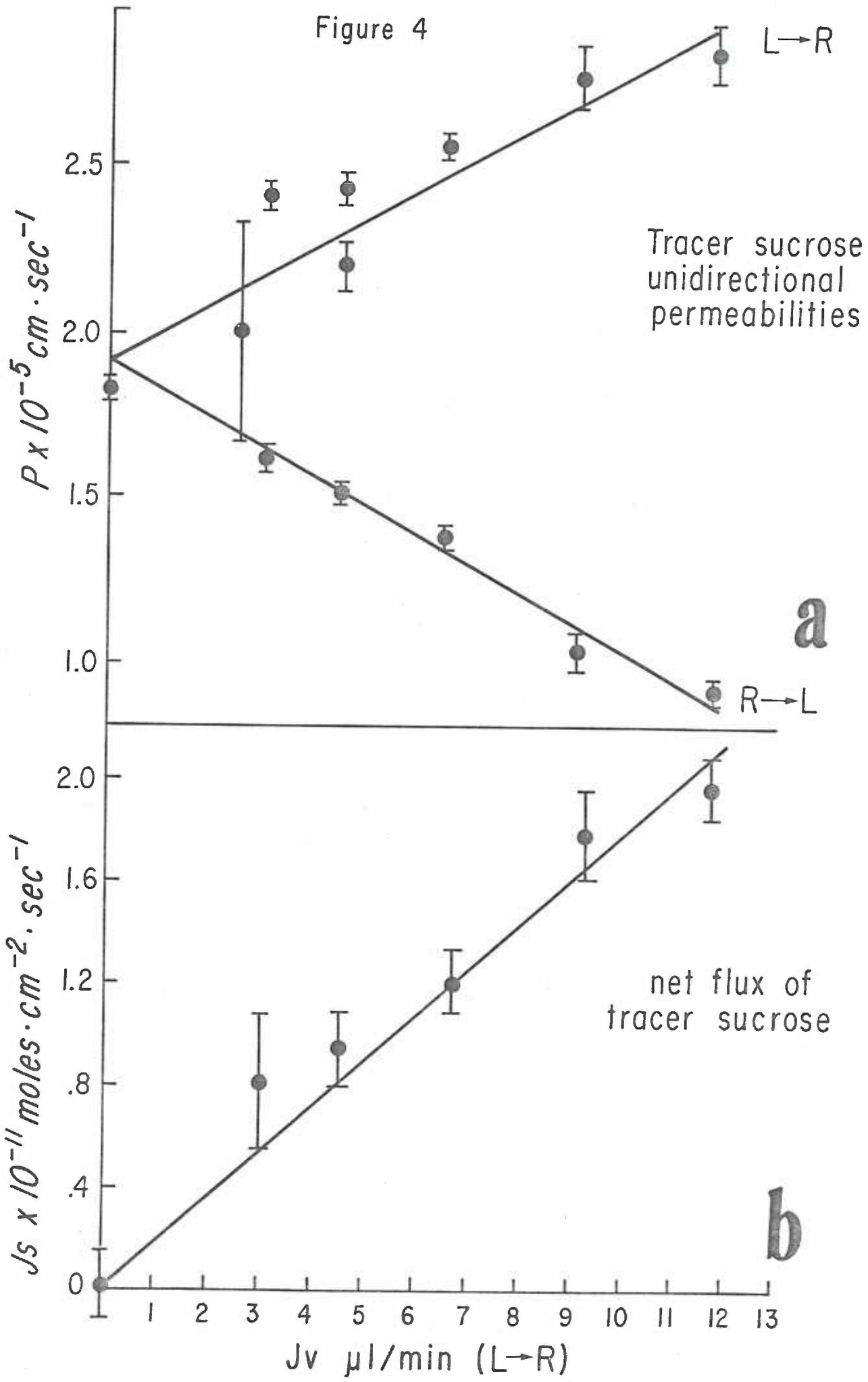
Figure 4
L→R
R→L
Tracer sucrose
unidirectional
permeabilities
P x 10⁻⁵ cm · sec⁻¹
2.5
2.0
1.5
1.0
a
net flux of
tracer sucrose
Js x 10⁻¹¹ moles · cm⁻², sec⁻¹
2.0
1.6
1.2
.8
.4
0
b
1 2 3 4 5 6 7 8 9 10 11 12 13
Jv µl/min (L→R)

opposite direction decrease. The lines drawn in the figure are best fit by the least squares method and have linear correlation coefficients of 0.92 and 0.98, respectively. The graph is symmetrical in that the slopes of the lines are equal in magnitude, but of opposite sign.

In figure 4b, the data from figure 4a is represented in terms of net fluxes of sucrose, calculated as mentioned previous (see page 32) and assuming 1 mmolal sucrose concentrations. As expected, the line intersects the ordinate at the origin, indicating no net flux of sucrose in the absence of a volume flow. Eliciting a volume flow with hydrostatic pressure is shown to result in a net flux of sucrose in the same direction as volume flow. A correlation coefficient of 0.95 for this data suggests that the relationship between volume flow and net solute flux is linear.

The equation derived by Kedem and Katchalsky (54) to describe solute fluxes across membranes can be applied to this data. This equation can be written as:

$$J_s = \omega\Delta\pi + J_v(1 - \sigma)\,\overline{C}_s$$

In the absence of an osmotic pressure gradient for the solute the equation reduces to:

$$J_s = J_v(1-\sigma)\,\overline{C}_s \qquad \Delta\pi = 0$$

In applying this latter equation to the data in figure 4b one must assume that unstirred layer effects are negligible. That this assumption is a good one will be discussed later. For now, use of the equation reveals that the slope of the line in figure 4b is related* to $(1 - \sigma)\,\overline{C}_s$ and, using 10^{-6} moles/gm. H_2O (1×10^{-3} molal) for $\overline{C}_s$, a value of 0.15 can be calculated for σ, the reflection coefficient of sucrose in this membrane.

---

* If the volume flow was expressed "per membrane area" the slope would equal $(1 - \sigma)\,\overline{C}_s$.

The next step of this experimentation was to combine the solvent drag effect with a solute drag effect. This is accomplished by experiments in which one of the membrane bathing solutions is made hypersomotic with respect to the other, and the flow of a tracer is monitored. The tracer can be chemically either the same as or different from the hyperosmotic species. With this experimental arrangement one would expect a volume flow across the membrane caused by the osmotic pressure difference,and a flux of the hyperosmotic agent across the membrane as if diffuses down its' chemical potential gradient. The movement of the tracer will thus be influenced by both solvent drag and solute drag. Of course, the solute drag effect will only be detectable if the hyperosmotic species is sufficiently permeable to the membrane and if the amount of interaction between the two solutes, quantitated by the interaction coefficient, λ, is large enough. The pertinent equation is:

$$J_s = J_v(1 - \sigma)\,\overline{C}_s + J_D\,\lambda\,\overline{C}_s \quad , \quad \Delta C_s = 0$$

where the second term describes the solute drag effect.

The first system to be evaluated was one in which the membrane was the S and S RC52, the hyperosmotic agent (driver) was sucrose, at 0.379 molal concentration on the left side of the membrane, and the tracer species was sucrose, placed alternately on the left and right sides of the membrane. The results of a series of experimental determinations of tracer permeabilities as a function of volume flow under these conditions is reported graphically in figure 5a.

FIGURE 5

a. In this series of experiments a 0.379 molal sucrose solution was in the left bathing chamber. The right bathing chamber contained pure water. Unidirectional tracer sucrose permeabilities are plotted against volume flow.

b. 0.189 molal sucrose solutions in both bathing chambers. Unidirectional tracer sucrose permeabilities plotted against volume flow.

c. Net flux of tracer sucrose plotted against volume flow. The top line was calculated from figure 5a.

A S and S RC52 membrane was used for these studies.

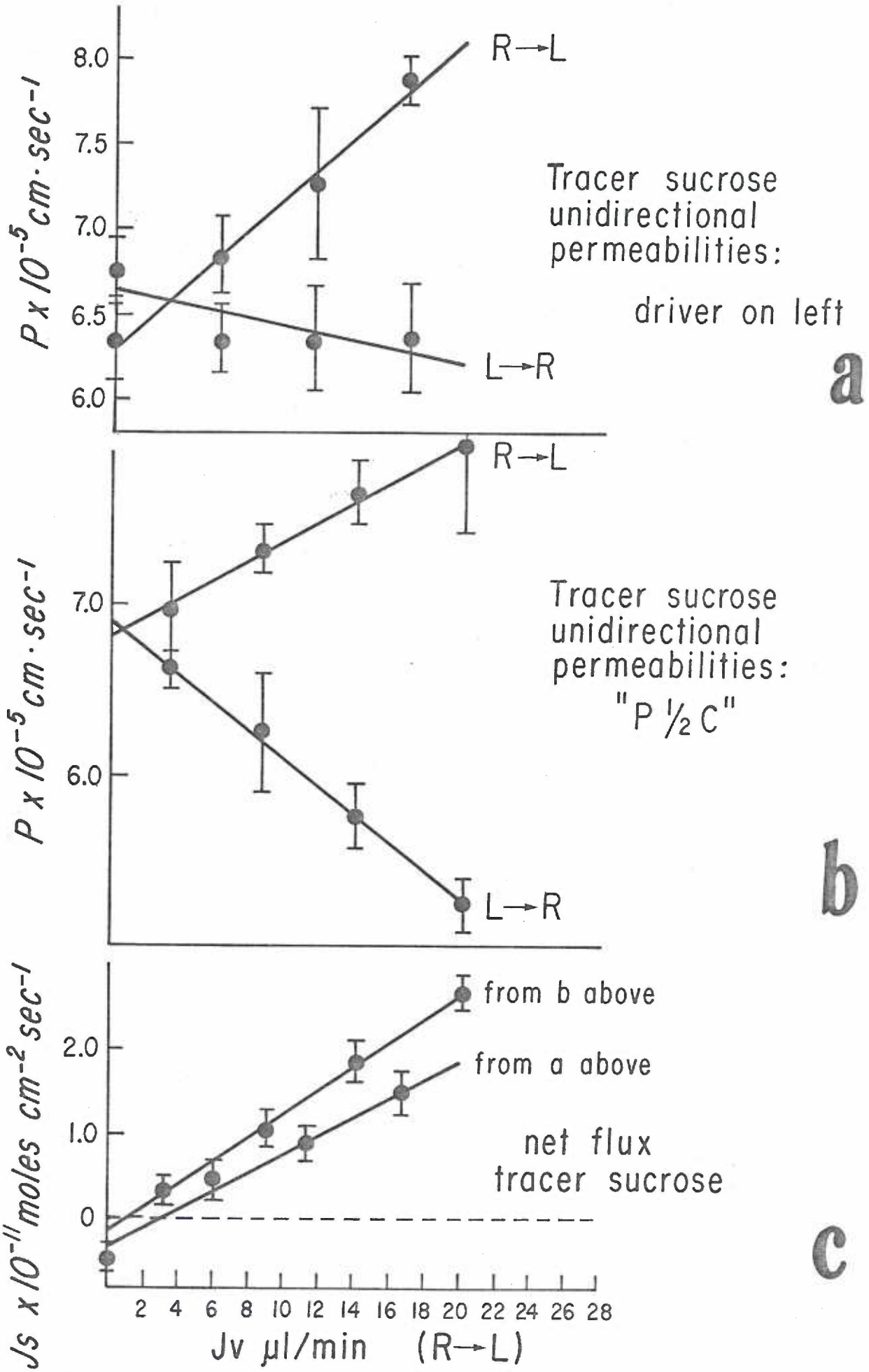
8.0
7.5
7.0
6.5
6.0
P x 10⁻⁵ cm·sec⁻¹
R→L
L→R
Tracer sucrose unidirectional permeabilities:
driver on left
a
7.0
6.0
P x 10⁻⁵ cm·sec⁻¹
R→L
L→R
Tracer sucrose unidirectional permeabilities:
"P ½ C"
b
2.0
1.0
0
Js x 10⁻¹¹ moles cm⁻² sec⁻¹
from b above
from a above
net flux tracer sucrose
c
2 4 6 8 10 12 14 16 18 20 22 24 26 28
Jv µl/min (R→L)

The upper line represents the unidirectional sucrose tracer permeabilities when the tracer is placed opposite to the hyperosmotic agent, on the right side of the membrane. In this case, the osmotic water flow will be in the same direction as tracer diffusion (R→L). It is thus expected that tracer permeabilities will increase with increasing J_v. The lower line represents the unidirectional sucrose tracer permeabilities when the tracer is placed on the same side as the hyperosmotic agent, on the left side. Again, as expected, an osmotic water flow has influenced the tracer flow. In this case opposing water flows decrease the tracer permeabilities.

Solute drag effects, if they exist, will be most readily identifiable at the point at which $J_v = 0$. At this point solvent flow influences on tracer diffusion will be absent and a difference between the L→R and R→L tracer permeabilities will be due to solute-solute interaction. Examination of figure 5a reveals that the L→R permeability line intersects the ordinate at 6.6×10^{-5} cm sec^{-1} while the R→L permeability line intersects somewhat lower, at 6.3×10^{-5}. Although these numbers are not statistically different at the $\rho = 0.05$ confidence level, this shift in permeabilities is in the direction one would expect if solute-solute flux coupling was a factor. The R→L line would be lowered by solute drag because in this series of experiments the tracer is diffusing in the direction opposite of hyperosmotic agent diffusion. Conversely the L→R line would be raised by solute drag because in these experiments the tracer and the hyperosmotic agent are diffusing in the same direction.

As a comparison, a series of "P 1/2 C" experiments were done,

In the figure 5b experiments, one half the concentration of the hyperosmotic agent from the previous experiments existed in both bathing solutions. The idea was to create a similar pore environment so that the two sets of data could be compared. Since experiments documented in figure 5a contain both solute and solvent drag effects while figure 5b experiments contain only solvent drag effects, any differences between the two will be due to solute drag effects.

To facilitate this comparison, the data from these two figures has been transformed into net fluxes in figure 5c. The top line was calculated from figure 5b data and the bottom line from figure 5a data. These two lines are not statistically different from one another in their slopes or in their ordinate intercepts at the p 0.05 confidence level. However, assuming that their ordinate intercepts were significantly different, one can use this information to calculate an interaction coefficient. The difference between ordinate intercepts is the net flux of solute caused by solute drag, $J_{s\ (J_D)}$. From the figure, this difference is 0.20×10^{-11} moles sec^{-1} cm^{-2}. The term that describes solute drag in equation (21) is:

$$J_{s(J_D)} = J_D \lambda \bar{C}_s$$

Using the experimentally determined value of 6.85×10^{-5} cm sec^{-1} for the permeability of the hyperosmotic agent, the flux of the driver, J_D, is found to be 2.60×10^{-5} cm sec^{-1}, and λ is calculated to equal 77 cm^3 $moles^{-1}$. Previous experience confirms that the amount of interaction suggested by this number is difficult to demonstrate experimentally.

Past work (17) in our laboratory has shown that the amount of solute-solute interaction depends partially upon the molecular sizes of the molecules involved and the size of the pores in the membrane. Therefore, it was decided that a solute drag component might be more readily demonstrated if some of these parameters were varied. Also, a greater contribution of solute drag would be expected if the flow of hyperosmotic agent was increased by increasing the concentration gradient for this species. These considerations led to the choice of solutes and concentrations chosen for further experiments on the combined effects of solute and solvent drag.

The data presented in figure 6 represents experiments in which two methods were used to increase the solute drag effect. First, the tracer size was enlarged with the use of raffinose instead of sucrose. Raffinose is a trisaccharide with a molecular radius 15 percent larger than that of sucrose. Secondly, a greater flow of hyperosmotic agent through the membrane was achieved by raising the concentration gradient for sucrose by 50%. This was done by increasing the concentration of sucrose from 0.379 molal as in the last experiments to 0.560 molal. The membrane used for these studies was the S and S AC62, which has experimental characteristics similar to those for the membrane used in the last series of experiments.

As before, figures 6a and 6b represent unidirectional tracer permeabilities. Figure 6a shows the case in which the left side bathing solution was hyperosmotic, while in figure 6b one half this concentration of hyperosmotic agent occupied both sides of the

FIGURE 6

a. In this series of experiments a 0.560 molal sucrose solution was in the left bathing chamber. The right bathing chamber contained pure water. Unidirectional tracer raffinose permeabilities are plotted against volume flow.

b. 0.263 molal sucrose solutions in both bathing chambers. Unidirectional tracer raffinose permeabilities plotted against volume flow.

c. Net flux of tracer raffinose plotted against volume flow. The top line was calculated from figure 5b and the bottom line from figure 5a.

A S and S AC62 membrane was used for these studies.

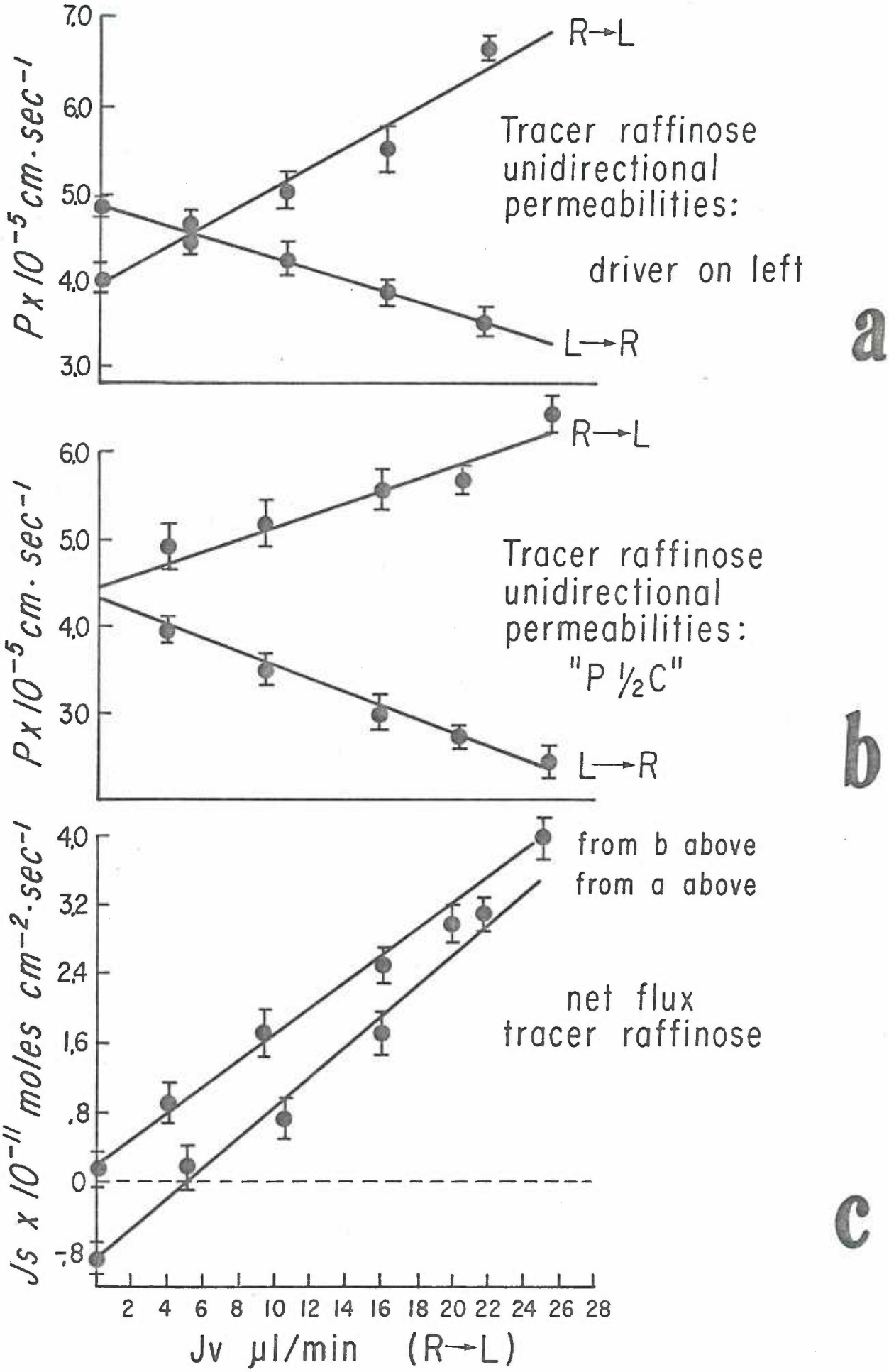
7.0
6.0
5.0
4.0
3.0
P x 10⁻⁵ cm · sec⁻¹
R→L
L→R
Tracer raffinose unidirectional permeabilities:
driver on left
a
6.0
5.0
4.0
3.0
P x 10⁻⁵ cm · sec⁻¹
R→L
L→R
Tracer raffinose unidirectional permeabilities:
"P ½C"
b
4.0
3.2
2.4
1.6
.8
0
-.8
Js x 10⁻¹¹ moles cm⁻² · sec⁻¹
from b above
from a above
net flux tracer raffinose
c
2 4 6 8 10 12 14 16 18 20 22 24 26 28
Jv µl/min (R→L)

membrane. The fact that the two lines in figure 6a do not meet on the ordinate clearly indicates the infuence of solute drag in these experiments. Volume flow effects are also observed. Figure 6b represents the volume flow effects without the influence of solute drag. This figure is analogous to figure 5b.

Data from figures 6a and 6b are compared in terms of net fluxes in figure 6c. The top line was calculated from figure 6b and represents net solute flux due to solvent drag alone. The bottom line was calculated from figure 6a data and represents net solute flux due to both solvent and solute drag. Assuming the difference between these two lines is wholly due to solute drag, an interaction coefficient for sucrose and raffinose in this membrane can be calculated. The P value for sucrose in this membrane is 4.85×10^{-5} cm sec^{-1} and λ is thus calculated to be 320 $moles^{-1}$ cm^{3}.

In order to assess a possible contribution of volume circulation effects as postulated by Patlak (18), experiments were done on a Nucleopore membrane 86. Good solute-solute interaction was obtained using PEG 600 as a hyperosmotic agent at 0.631 molal concentration when sucrose was chosen as the tracer. Three graphs are presented in figure 7 which are analogous to those in figures 5 and 6. The permeability coefficient of the hyperosmotic agent, PEG600, was determined to be 0.730×10^{-5} cm sec^{-1} in this membrane. From this, and the difference in net fluxes between the two lines in figure 7c, an interaction coefficient of 750 was calculated.

Since work in biological systems has often utilized urea as

FIGURE 7

a. In this series of experiments a 0.631 molal PEG 600 solution was in the left bathing chamber. The right bathing chamber contained pure water. Unidirectional tracer sucrose permeabilities are plotted against volume flow.

b. 0.283 molal PEG 600 solutions are in both bathing chambers. Unidirectional tracer sucrose permeabilities are plotted against volume flow.

c. Net flux of tracer sucrose plotted against volume flow. The top line was calculated from figure 7b and the bottom line from figure 7a.

A Nucleopore membrane was used.

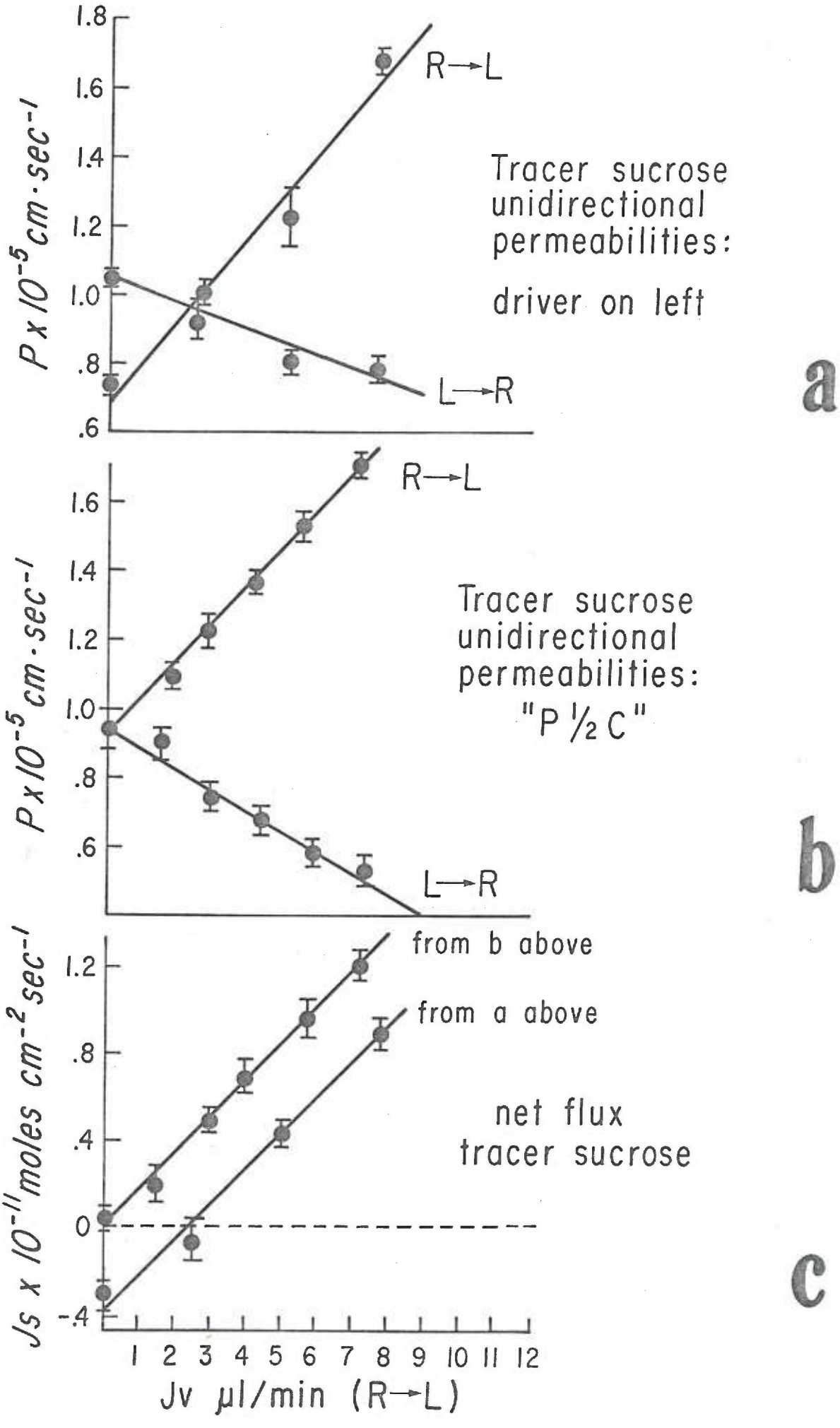
1.8
1.6
1.4
1.2
1.0
.8
.6
P x 10⁻⁵ cm·sec⁻¹
R→L
L→R
Tracer sucrose unidirectional permeabilities:
driver on left
a
1.6
1.4
1.2
1.0
.8
.6
P x 10⁻⁵ cm·sec⁻¹
R→L
L→R
Tracer sucrose unidirectional permeabilities:
"P ½ C"
b
1.2
.8
.4
0
-.4
Js x 10⁻¹¹ moles cm⁻² sec⁻¹
from b above
from a above
net flux tracer sucrose
c
1 2 3 4 5 6 7 8 9 10 11 12
Jv µl/min (R→L)

as a hyperosmotic agent it was decided to try this solute in the artificial membrane system. To maximize potential solute drag effects a membrane with smaller pores was chosen, the S and S RC5l with "pores" of about 35 Å radius. Also, the high solubility of urea in water allowed the use of a large concentration gradient, maximizing the trans-membrane flow of urea. Preliminary experiments with 2.0 molal concentration gradient for urea across the membrane with sucrose as the tracer species did not show significant solute drag flux asymmetries. These experiments were not continued.

DISCUSSION

Passive mechanisms of solute transfer across epithelial tissues have received renewed interest in recent years. Studies by Diamond and Fromter (77,74) have demonstrated that small molecules may traverse epithelia of various types by an extracellular route involving cell-to-cell tight junctions and that this route, in some tissues, can furnish a major pathway for solute permeation. Studies by Fordtran et al.(29) on the human small intestine and by Levitt et al.(72) on the dog jejunum have demonstrated that forces influencing passive movement of salt, water and some sugars play a major role in this tissue. Berry and Boulpaep (73) have documented a role for passive transport of nonelectrolytes through a paracellular pathway of the in vivo proximal tubule of the Necturus kidney. Passive permeation of the Necturus gall bladder has also been studied. (74)

Further interest in passive transport across membranes was generated by the discovery of Ussing (1) and by Franz and Van Bruggen (4) of an anomolous net transport of small molecules through amphibian skin under the influence of outside bathing solution hypertonicity. The independence of this phenomena from epithelial cell metabolism indicated to these later workers that a passive mechanism of solute transfer through the skin was involved. Subsequent work in our laboratory has shown the phenomena to occur in artificial membranes, confirming a passive explanation. More recently, Leif and Essig (24) have detected similar anomolous net transport of urea in

the toad bladder and Mullen, in our laboratory (unpublished results) has detected the influences of anomolous solute transport in amphibian intestine.

Such studies of the mechanisms of membrane transport invariably lead to discussions of the forces responsible for the observed solute movement. With this approach it has been possible to explain experimental observations in some systems and predict effects in others. The force responsible for the anomolous net transport of solutes across membranes has been shown to originate from a flow of hyperosmotic agent through the membrane. If there happens to be a volume flow across the membrane, this also has been shown (78, 72) to influence solute movement by solvent drag, and can be thought of as a second force. Of course, if a chemical potential gradient exists for the solute across the membrane, this will represent a third force. To describe a passive transport system containing two or more solutes, one must include accounts of all these forces. An equation designed to provide such a description for the case of a two solute system has been presented in this thesis and is rewritten here as

$$J_s = P_s \Delta C + J_v (1 - \sigma) \bar{C}_s + J_D \lambda \bar{C}_s \qquad (21)$$

where the three terms in the equation were formulated to account for the three forces; diffusion, solvent drag and solute drag, respectively. The experiments reported in this thesis provide a test for the usefulness of this equation in describing the mechanisms of passive transport across membranes.

Before discussing specific results, a few comments may be

made on the potentially confusing influences of unstirred layers. Briefly, these effects come into play if the concentration of solute next to the membrane is not the same as the concentration of solute in the bulk solution. Previous work in our laboratory (23) has attempted to evaluate the contribution of unstirred layer effects to the results of permeability determinations on our synthetic membrane systems. The approach used was one developed by Ginsburg and Katchalsky (65) and involves the comparision of experimental and calculated permeabilities of a solute such as THO. The calculated permeability coefficient was determined by:

$$P = \frac{n\pi d^2 D}{4h} \qquad (27)$$

where n equals pore density, d equals pore diameter, D is the diffusion coefficient of the solute and h is the membrane thickness. The values of n and d were determined by electron microscopy of the Nucleopore membrane. To determine the unstirred layer thickness the following equation was used:

$$\frac{1}{\omega'} = \frac{1}{\omega} + \frac{2RT}{D}\,\delta \qquad (28)$$

where ω' is the experimental permeability coefficient, and δ is the thickness of the unstirred layer. Using this method, the theoretical and experimental permeabilities of THO, urea, mannitol, sucrose and inulin were found to be identical within the usual limits of error of these measurements. Thus, unstirred layer effects probably present no major problem in the current studies.

The first phase of the experimentation involved an

evaluation of the validity of the solvent drag term of equation 21. This term, $J_v (1 - \sigma) \bar{C}_s$, makes certain qualitative and quantitative predictions as to the nature of solvent-solute interaction. The first to be considered is the prediction of this term that the solvent drag effect will be linearly related to volume flow. When unidirectional tracer permeabilities are being measured, this means that these P values should increase or decrease linearly with volume flow. In studies of this type (see figure 4a) this was found to hold true. The line drawn from R→L unidirectional permeability determinations is linear, with a correlation coefficient of r = 0.92 and the corresponding L→R permeability line is also linear, with r equal to 0.98. Of course, the net solute flux versus volume flow , graph (4b), is also linear since these values were calculated from those in figure 4a.

Intuitively it is evident that a linear relationship cannot continue at high rates of volume flow. Consider the experiment in which a volume flow is occurring in a direction opposite that of a diffusing tracer solute. Initially, no tracer exists on the side of the membrane from which the volume flow originates. As the rate of volume flow increases the permeability coefficients determined for the movement of the tracer will decrease. If this decrease continued in a linear manner, a volume flow would eventually be reached where the corresponding permeability coefficient was negative, clearly an impossible situation. In actuality, then, the relationship between the solvent drag effect and the volume flow must become nonlinear

at increasingly high volume flows. This effect would be manifest in figures 4a and 4b as decreasing slopes with increasing volume flow rates. As this does not occur, the volume flows utilized in these experiments were not sufficient for this inconsistency in the solvent drag term to be of importance. Since in vivo volume flows are generally less than those reported here, this problem is of even less consequence in biological membranes. (40)

Another prediction of the solvent drag term in equation 21 is that the effect will be symmetrical. That is, a certain volume flow will cause a decrease in an opposing unidirectional tracer permeability that will be equal to the increase the same volume flow will cause in the unidirectional permeability for a tracer diffusing in the same direction as the volume flow. This may not be immediately apparent from equation 21, which is written for net fluxes of solute, but becomes clear when one considers that this equation also applies to unidirectional tracer permeabilities as follows:

$$J_{s\ R\to L} = P_s \Delta C + J_v (1 - \sigma) \overline{C}_s$$

$$J_{s\ L\to R} = P_s \Delta C - J_v (1 - \sigma) \overline{C}_s \qquad J_D = 0$$

dividing both equations by the tracer concentration gives:

$$P_{R\to L} = P_s + J_v (1 - \sigma)/2 \tag{29}$$

$$P_{L\to R} = P_s - J_v (1 - \sigma)/2 \tag{30}$$

thus, a volume flow will have an equal but opposite effect on the two tracer permeabilities, $P_{R\to L}$ and $P_{L\to R}$. This effect is defined by

$J_v(1 - \sigma)/2$. To this end, one can see that the experimental solvent drag effect reported in figure 4a is symmetrical and the absolute values of the slopes of the R→L and L→R tracer permeability lines are equal to within 3%.

The preceding paragraphs have cited evidence that the solvent drag term in equation 21 is a good qualitative representation of the volume flow effect created in the artifical membrane system. Quantitatively, however, there appears to be a discrepancy. The fact that the solvent drag term contains the reflection coefficient, σ, allows a calculation of this value. Determinations of this type are commonly done in biological membranes (29, 72). The following relation, obtained from equation 21 can be used:

$$1 - \frac{J_{s(J_v)}}{\overline{C}_s J_v} = \sigma \qquad (31)$$

where $J_{s(J_v)}$ is the net flux of the solute due to solvent drag. Applying this relation to the data in figure 4b, a reflection coefficient of $0.15 \pm .10$ is calculated for sucrose in this membrane. Using another method, that which compares observed and calculated osmotic pressures for a sucrose concentration gradient across the membrane, a value of 0.02 is calculated for the reflection coefficient. The origin of the discrepancy between these two values is unknown. If 0.02 is taken to be the more accurate estimate, then the $0.15 \pm .10$ result would mean that not as much sucrose is being "dragged" through the membrane by volume flow as the theory predicts, that is, more is being "reflected" that a σ of 0.02 would indicate. However, the large

standard error inherent in the value of the reflection coefficient calculated from equation 31 precludes the formulation of detailed theories as to a possible discrepancy. More experimentation is needed.

The next phase of the experimentation involved observing the combined effects of solvent drag and solute drag on the flux of a tracer across a membrane. The experiments reported in figure 5, 6, and 7 serve this purpose. Recall that these experiments were designed in light of two specific questions: Is one effect of such quantitative proportions as to render the other effect of little importance? And, if not, are the two effects adequately described by equation 21?

The creation of a solute drag effect was attempted with four different pairs of solutes. In the experiments of figure 5a, sucrose was used as both the hyperosmotic agent and the tracer species, and an interaction coefficient of 77 moles^{-1} cm^{3} was calculated. As noted previously, this amount of interaction is not statistically significant. When a larger tracer was used, the amount of solute-solute interaction increased. Figure 6a shows the results of this experiment. With raffinose as the tracer species, the calculated interaction coefficient increased to 320 moles^{-1} cm^{3}. It must be noted, however, that different pieces of membranes were used in these two studies. Although the membranes were thought to be similar, their differences might have contributed to the observed increase in interaction. A third set of experiments utilized a homopore membrane, with sucrose as the tracer species and PEG 600 as the hyperosmotic agent. This experimentation is recorded in figure 7a. With this combination

of membrane, tracer and hyperosmotic agent the calculated interaction coefficient has increased even further to 720 moles^{-1} cm^{3}. Preliminary experiments with urea as a hyperosmotic agent and sucrose as the tracer on the homopore membrane showed no detectable solute-solute interaction effects. This result is probably due to the small molecular size of urea in relation to the size of the pores in the membrane used. The overall relationship between the molecular sizes of the solutes involved and the extent of the solute-solute interaction is in accord with earlier results of Galey (32) in this laboratory. Further, the demonstration of significant solute drag effects on the homoporous Nucleopore 86 membrane rules out the involvement of volume circulation as described by Patlak and Rapoport (18).

To evaluate the relationship between solvent drag and solute drag effects, the part "c" graphs of figures 6 and 7 should be consulted. Recall that the lower line in these figures (the one labelled "from a above") represents the net flow of a solute, for which there is no concentration gradient, under the influence of both solute and solvent drag. Recall also that the upper line (labelled "from b above") represents the net flow of the same solute but under the influences of only solvent drag. Since the solute drag term of equation 21 does not contain a volume flow factor this equation predicts that the effect of solute drag will remain constant with changing volume flow rates. First, consider figure 7c. At zero net volume flow, the net sucrose flux shown on the"from a above" line is due wholly to solute drag and equals -0.4×10^{-11} moles cm^{-2} sec^{-1}. At 7 ul/min

the net flux of sucrose due to solvent drag can be read off the "from b above" line and equals 1.2 x 10^{-11} moles cm^{-2} sec^{-1}. However, the net flux of solute at 7 ul/min when both forces are operative has been reduced from this value by the solute drag effect. Read off the "from a above line" this net flux equals 0.8 x 10^{-11} moles cm^{-2} sec^{-1}. It can be seen that the solute drag component has remained at -0.4 x 10^{-11} moles cm^{-2} sec^{-1}, despite changes in volume flow rates.

The agreement between theory and observation is not quite as good for the experiments on the heteropore membrane shown in figure 6c. In these studies the solute drag effect appears to diminish with increasing volume flow. At zero volume flow the value equals about-0.8 x 10^{-11} moles cm^{-2} sec^{-1}, while at 25 ul min^{-1} volume flow the value equals about -0.4 x 10^{-11} moles cm^{-2} sec^{-1}. The origin of this apparent relationship between volume flow rate and the solute-solute interaction effect is unknown. It is probably the case that more deviation from the theory is seen in this latter case because a larger range of volume flow rates is covered during the experiments. It is reasonable to assume that in vivo, where the range of flow rates observed is much smaller, the solute drag effect would remain approximately constant.

The answers to the questions posed above can now be discussed. The evidence suggests that depending on the identity of the solutes, solute drag effects can assume significant proportions, and that these effects will remain, to the first approximation,

independent of other influences on solute flux, such as solvent drag. This information tends to confirm the usefulness of equation 21 as a method of describing the passive flow of solutes across membranes.

SUMMARY AND CONCLUSIONS

This thesis reports on the individual and combined effects of solvent drag and solute drag on the passive diffusion of nonelectrolytes across synthetic membranes. The data shows that the solvent drag effect is qualitatively well explained by the corresponding term in the equation first derived by Kedem and Katchalsky for passive solute flux across membranes. Quantitatively, there appears to be a discrepancy between theory and observation. Further experimentation is needed to establish the source and extent of this discrepancy.

The effects of solute drag are demonstrated to be dependent upon the molecular sizes of the solutes involved, confirming previous results. Further, the data shows that solvent and solute drag effects act independently and additively in influencing the passive flow of solutes across membranes. It is thought that in vivo, both of these potential forces are operative on the movement of biologically important molecules across epithelia.

REFERENCES

1. Ussing, H.H. 1966. Anomolous transport of electrolytes and sucrose through the isolated frog skin induced by hypertonicity of the outside bathing solution. Ann. N.Y. Acad. Sci. 137, 543-555.

2. Ussing, H.H. 1969. The interpretation of tracer fluxes in terms of membrane structure. Quant. Rev. Biophys. 1:4.

3. Franz, T.J., Galey, W.R., and Van Bruggen, J.T. 1968. Further observations on asymmetrical solute movement across membranes. J. Gen. Physiol. 51:1.

4. Franz, T.J., and Van Bruggen, J.T. 1967. A possible mechanism of action of DMSO. Ann. N.Y. Acad. Sci. 141 : 302

5. Barnes, T.C. 1939. The influence of heavy water and temperature on the electrical potential of frog skin. J. Cell. and Comp. Physiol. 13:39.

6. Ussing, H. H., and Windhager, E. E. 1964. Nature of shunt pathway and active transport path through frog skin epithelium. Acta Physiol. Scand. 61:484.

7. Lindley, B. D., Hoshiko, T., and Leb, D.E. 1964. Effects of D_2O and osmotic gradients on potential and resistance of the isolated frog skin. J. Gen. Physiol. 47:773.

8. Franz, T.J., and Van Bruggen, J.T. 1967. Hyperosmolarity and the net transport of nonelectrolytes in frog skin. J. Gen. Physiol. 50:993.

9. Ussing, H. H. 1965. Relationship between osmotic reactions and active sodium transport in the frog skin epithelium. Acta Physiol. Scand. 63:141.

10. Ussing, H. H. 1967 Active Na transport across the frog skin epithelium and its relation to epithelial structure. Ber. Bunsenges Physitcal. Chem. 71:807.

11. Ussing, H. H. and B. Johansen. 1969. Anomolous transport of sucrose and urea in toad skin. Nephron. 6:317.

12. Biber, T. U. L. and Curran, P. F. 1968. Coupled solute fluxes in frog skin. Biophys. J. 8:A127.

13. Allbright, J.G., and R. Mills. 1965. A study of diffusion in the ternary system, labelled urea-urea-water, at 25° by measurement of the intradiffusion coefficients of urea. J. Phys. Chem. 69:3120.

14. Ellerton, H.D., and P. J. Dunlop. 1967. Diffusion and frictional coefficients for four compositions of the system water-sucrose-mannitol at 25°. J. Phys. Chem. 71:1291.

15. Dunlop, P. J. 1957. Interacting flows in diffusion of the system raffinose-urea-water. J. Phys. Chem. 61:1619.

16. Ellerton, H. D. and Dunlop, P. J. 1967. Ternary diffusion and frictional coefficients for one composition of the system water-urea-sucrose at 25° . J. Phys. Chem. 71:1538.

17. Galey, W. R. and Van Bruggen, J. T. 1970. The coupling of solute fluxes in membranes. J. Gen. Physiol. 55:220.

18. Patlak, C. S. and Rapoport, S. I. 1971. Theoretical analysis of net tracer flux due to volume circulation in a membrane with pores of different sizes. Relation to solute drag model. J. Gen. Physiol. 57:113.

19. Sollner, K. 1945. The physical chemistry of membranes with particular reference to the electrical behavior of membranes of porous character. III. J. Phys. Chem. 49:265.

20. Rapoport, S. I. 1966. Convection, diffusion, and electrical current through a membrane. Acta Physiol. Scand. 66:385.

21. Goldstein, D.A., and Solomon, A.D. 1960. Determination of equivalent pore radius for human red cells by osmotic pressure measurement. J. Gen. Physiol. 44:1.

22. Paganelli, C. V. and Solomon, A. K. 1957. The rate of exchange of tritiated water across the human red cell membrane. J. Gen. Physiol. 41:259.

23. Van Bruggen, J. T., Boyett, J. D., Van Bueren, A. L. and Galey, W. R. 1974. Solute flux coupling in a homopore membrane. J. Gen. Physiol. 63:639.

24. Lief, P. D. and Essig, A. 1973. Urea transport in the toad bladder; coupling of urea flows. J. Membrane Biol. 12:159.

25. Ussing, H. H. 1952. Some aspects of the application of tracers in permeability studies. Advances in Enzymology. 13:21.

26. Ussing, H. H., and Anderson, B. 1955. The relation between solvent drag and active transport of ions. Proc. IIIrd Int. Congr. Biochem. Brussels. New York : N.Y. : Academic Press. 434.

27. Anderson, B., and Ussing, H. H. 1957. Solvent drag on non-electrolytes during osmotic flow. 39:228.

28. Urakabe, S., Handler, J. S., Orloff, J. 1970. Effect of hypertonicity of permeability properties of the toad bladder. Amer J. Physiol 218:1179.

29. Fordtran, J. S., Rector, F. C., Ewton, M. F., Soter, N., and Kinney, J. 1965. Permeability characteristics of the human small intestine. J. Clin. Invest. 44:1935.

30. Hakim, A. A., and Lifson, N. 1964. Urea transport across dog intestinal mucosa in vitro. Am. J. Physiol. 206:1315.

31. Turnberg, L. A. 1971. Potassium transport in the human small bowel. Gut. 12:811.

32. Galey, W. R. 1969. Coupled solute fluxes in membrane systems. Univ. of Ore. Med. School. Unpublished doctoral dissertation.

33. Renkin, E. M. 1952. Capillary permeability to lipid-soluble molecules. Am. J. Physiol. 168:538.

34. Holter, H. 1962. Pinocytosis. In G.W. Wolstenholme (ed.) Ciba Found. Symp. : Enzyme and drug action. Boston, Mass. : Little, Brown and Co.

35. Palade, G. E. 1960. Transport in quanta across the endothelium of blood capillaries. Anat. Rec. 136:254.

36. Ussing, H. H., Erlij, D. Lassen, U. 1974. Transport pathways in biological membranes.

37. Koefoed-Johnsen, V., Ussing, H. H. 1953. The contributions of diffusion and flow to the passage of D_2O through living membranes. Effect of neurohypophyseal hormone on isolated anuran skin. Acta Physiol. Scand. 28:60.

38. Curan, P. F. 1973. Amino acid transport in intestines. In Transport Mechanisms in Epithelia. Ed. by H.H. Ussing and N.A. Thoru. Munksgaard, Cophenhagen.

39. Lifson, N., Hakim, A. A. 1966. Simple diffusion convective model for intestinal absorbtion of a non electrolyte (urea) Am. J. Physiol. 211:1137.

40. Mullen, T. Personal communication.

41. MacRobbie, E.A.C., Ussing, H. H. 1961. Osmotic behavior of epithelial cells of frog skin. Acta Physiol. Scand. 53:348.

42. Farquhar, M.G. and Palade, G.E. 1963. Junctional complexes in various epithelia. J. Cell Biology. 17:375.

43. McNutt, N. S. and Weinstein, R. S. 1973. Membrane ultrastructure at mammalian intercellular junctions. In Progress in Biophysics. Ed. by J. Butler and D. Noble. Oxford. p. 44.

44. Diamond, J. M. 1977. The epithelial junction : bridge, gate and fence. The Physiologist. 20:10.

45. DiBona, D. R. 1972. Passive intercellular pathways in amphibian epithelia. Nature New Biology. 8:9.

46. Fick, A. 1855. Ueber diffusion. Paggend. Ann. 94:59.

47. Schultz, S.G. 1976. Transport across epithelia : some basic principles. Kidney International 9:65.

48. Einstein, A. 1956. Investigations on the theory of the Brownian movement. 1905. (English translation and notes by R. Farth. Reprint: Dover, New York.

49. Einstein, A. 1905. On the movement of small particles suspended in a stationary liquid demanded by the molecular-kinetic theory of heat. Ann. Physik. 17:549.

50. Einstein, A. 1906. On the theory of the Brownian movement. Ann. Physik. 19:371.

51. Van't Hoff, J. H. 1887. Die Rolle des osmotichen Druches in der anologie zwichen Losungen und Gasen. Physikal Chem. 1:481.

52. Staverman, A. J. 1952. Non-equilibrium thermodynamics of membrane processes. Trans. Faraday Soc. 48:176.

53. De Groot, S. R. 1963. Thermodynamics of irreversible processes. Amsterdam : North Holland Publishing Co.

54. Kedem, O., and Katchalsky, A. 1958. Thermodynamic analysis of the permeability of biological membranes to non-electrolytes. Biochim. Biophys. Acta. 27:229.

55. Onsager, L. 1931. Reciprocal relations in irreversible processes. Phys. Rev. 37:405.

56. Staverman, A. J. 1951. Theory of measurement of osmotic pressure. Rec. Trav. Chim. 70:344.

57. Stein, W.D. 1967. The movement of molecules across biological membranes. New York : Academic Press. 41-48.

58. Price, P.B. and Walker, R.M. 1962. Electron microscope observation of etched tracks from spallation recoils in mica. Phys. Rev. Lett. 8:217.

59. Price, P. B. and Walter, R. M. 1962. Chemical etchings of charged-particle tracks in solids. J. Appl. Phys. 33:3407.

60. Fleischer, R. L., Price, P. B., Walker, R. M., and Hubbard, E. L. 1964. Track registration in various solid-state nuclear track detectors. Phys. Rev. 133:A1443.

61. Bean, C. P., Doyle, M. V. and Entine, G. 1970. Etching of sub-micron pores in irradiated mica. J. Appl. Phys. 41:1454.

62. Pappenheimer, J. R., Renkin, E. M. and Borreo, L. M. 1951. Filtration, diffusion and molecular sieving through peripheral capillary membranes. A contribution to the pore theory of capillary permeability. Am. J. Physiol. 167:13.

63. Riley, R., Gardner, J. O., and Merten, U. 1964. Cellulose acetate membranes : electron microscopy of structure. Science. 143:801.

64. Renkin, E. M. 1954. Filtration, diffusion and molecular sieving through porous cellulose membranes. J. Gen. Physiol. 38:225.

65. Ginzburg, B. Z., and Katchalsky, A. 1963. Frictional coefficients of the flow of non-electrolytes through artificial membranes. J. Gen. Physiol. 47:403.

66. Hays, R. M., and Leaf, A. 1962. Studies on the movement of water through the isolated toad bladder and its modification by vasopressin. J. Gen. Physio. 45:933.

67. Rosenberg, T., and Wildbrandt, W. 1957. Uphill transport induced by counterflow. J. of Gen. Physiol. 41:289.

68. Froemter, E., Rumrich, G., and Ullrich, K.J. 1973. Phenomenologic description of Na^+, Cl^- and HCO_2 absorption from proximal tubules of the rat kidney. Pfleugers Arch. Eur. J. Physiol. 343:189.

69. Ochsenfahrt, H. and Winne, D. 1973. The contribution of solvent drag to the intestinal absorption of tritiated water and urea from the jejunum of the rat. Naunym-Schmiedeberg's Arch. Pharmacol. 279:133.

70. Ochsenfahrt, H., and Winnd, E. 1974a. The contribution of solvent drag to the intestinal absorption of the basic drugs amidophyrine and antipyrine from the jejunum of the rat. Naunym-Schmiedeberg's Arch. Pharmacol. 281:175.

71. Ochsenfahrt, H., and Winne, D. 1974b. The contribution of solvent drag to the intestinal absorption of the acidic drugs benzoic acid and salicylic acid from the jejunum of the rat. Naunyn-Schmiedeberg's Arch. Pharmacol. 281:197.

72. Levitt, D. G., Hakim, A. A. and Lifson, N. 1969. Evaluation of components of transport of sugars by dog jejunum in vivo. Am. J. Physiol. 217:777.

73. Berry, C. A., and Boulpaep, E. L. 1975. Nonelectrolyte permeability of the paracellular pathways in Necturus proximal tubule. Am. J. Physiol. 228:581.

74. Fromter, E. 1972. The route of passive ion movement through the epithelium of Necturus gall bladder. J. Memb. Biol. 8:259.

75. Durbin , R. P. 1960. Osmotic flow of water across permeable cellulose membranes. J. Gen. Physiol. 44:315.

76. Bentzel, C.J., Davies, M., Scott, W. N., Zatzman, M., Solomon, A. K. 1968. Osmotic flow in the proximal tubule of Necturus kidney. J. Gen. Physiol. 51:517.

77. Fromter, E. and Diamond, J. M. 1972. Route of passive ion permeation in epithelia. Nature New Biology. 235:9.

78. Ussing, H. H., Kruhoffer, P., Thayson, Hess, and Thorn, N. A. 1969. The alkali metal ions in biology. Springer, Berlin.

APPENDIX

The following data from an actual experiment will serve to illustrate the method of calculation of all flux experiments.

Experiment 132-156 (See figure 6, $J_v = 0$)

membrane: S and S, AC62

volume flow: 0.0 (stopped with 32.5 cm. Hg hydrostatic pressure applied to left bathing chamber)

left chamber solution contents: 0.560 molal sucrose 4,639,960 DPM/ml $(5{,}103{,}960 \frac{\text{DPM}}{\text{gm } H_2O})^3$ H-raffinose

right chamber solution contents: H_2O chamber volume, 9.31 ml.

sample time	DPM in 0.150 ml sample of receiving chamber	calculated P
4 min.	3,365	--
6	7,251	4.99×10^{-5} cm/sec
8	10,876	4.73
10	14,738	5.10
12	18,272	4.77
14	21,885	4.94

average = 4.91×10^{-5} cm/sec

$\pm$ 1 S.D. = 0.15×10^{-5}

P values were calculated with equation 22 on page 31. The activity of the tracer in the donor solution, Ad, was estimated by using the disintegrations per minute of the radioactive tracer per gram of water. In experiment 132-156 this value is 5,103,960 DPM/gm H_2O. The membrane area, Ma, is 8 cm^2 and the sample time is 120 seconds. The

change in activity in the receiving chamber is calculated according to the equation at the bottom of page 31. Below I have inserted the appropriate values from experiment 132-156 to calculate ΔA for the first time interval.

$$\Delta A = \frac{(7251 \text{ DPM})\ (9.31 \text{ cm}^3)}{(0.150 \text{ cm}^3)} - \frac{(3365 \text{ DPM})\ \left[(9.31 \text{ cm}^3) - (0.150 \text{ cm}^3)\right]}{(0.150 \text{ cm}^3)}$$

$$= 2.44 \times 10^{-5} \text{ DPM}$$

The permeability coefficient calculated by equation 22 then equals:

$$P = \frac{2.44 \times 10^{-5} \text{ DPM}}{(120 \text{ sec})\ (8\text{cm}^2)\ (5{,}103{,}960 \text{ DMP/cm}^3)}$$

$$= 4.99 \times 10^{-5} \text{ cm/sec}$$